HHS Public Access

Author manuscript

J Neuroimmunol. Author manuscript; available in PMC 2019 October 15.

Published in final edited form as:

J Neuroimmunol. 2018 October 15; 323: 152–166. doi:10.1016/j.jneuroim.2018.06.019.

Lower level noise exposure that produces only TTS modulates the immune homeostasis of cochlear macrophages

Mitchell D. Frye, **Celia Zhang**, and **Bo Hua Hu***

Center for Hearing and Deafness, University at Buffalo, 137 Cary Hall, 3435 Main Street, Buffalo, NY 14214, USA

Abstract

Noise exposure producing temporary threshold shifts (TTS) has been demonstrated to cause permanent changes to cochlear physiology and hearing function. Several explanations have been purported to underlie these long-term changes in cochlear function, such as damage to sensory cell stereocilia and synaptic connections between sensory cells and their innervation by spiral ganglion neurons, and demyelination of the auditory nerve. Though these structural defects have been implicated in hearing difficulty, cochlear responses to this stress damage remains poorly understood. Here, we report the activation of the cochlear immune system following exposure to lower level noise (LLN) that causes only TTS. Using multiple morphological, molecular and functional parameters, we assessed the responses of macrophages, the primary immune cell population in the cochlea, to the LLN exposure. This study reveals that a LLN that causes only TTS increases the macrophage population in cochlear regions immediately adjacent to sensory cells and their innervations. Many of these cells acquire an activated morphology and express the immune molecules CCL2 and ICAM1 that are important for macrophage inflammatory activity and adhesion. However, LLN exposure reduces macrophage phagocytic ability. While the activated morphology of cochlear macrophages reverses, the complete recovery is not achieved 2 months after the LLN exposure. Taken together, these observations clearly implicate the cochlear immune system in the cochlear response to LLN that causes no permanent threshold change.

Graphical Abstract

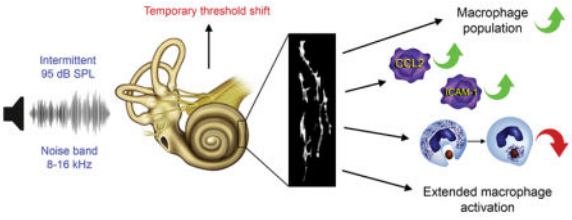

*Corresponding author: Bo Hua Hu, Ph.D., Center for Hearing and Deafness, State University of New York at Buffalo, Buffalo, NY 14214, USA, Phone: 001-716-829-5316; Fax: 001-716-829-2980, bhu@buffalo.edu.

Disclosure

The authors declare no conflict of interest.

Keywords

Macrophage; Cochlea; Lower level noise; Temporary threshold shift; Immunity; Inflammation

1 Introduction

It has long been established that exposure to high-intensity noise compromises sensory cell viability and produces permanent hearing loss (Hamernik et al., 1980; Hamernik et al., 1984; Henderson et al., 1998; Hu, 2012; Hu et al., 2000; Saunders et al., 1985; Sulkowski et al., 1981; Taylor et al., 1965). Although high-level noise has been shown to cause the loss of cochlear cells and sensory cells in particular, low-intensity noise is more prevalent in real world circumstances. Though many individuals living in an industrial society may encounter high-intensity noise only on an infrequent basis, those same individuals are nevertheless likely to be exposed to longer durations of a lower-level noise (LLN) that causes only a temporary hearing loss. Even without permanent hearing loss, individuals who sustain LLN exposure can display signs of auditory symptoms. Such dysfunction includes difficulty in speech perception in noisy conditions, tinnitus, hyperacusis and auditory processing disorders (Bharadwaj et al., 2015; Hickox et al., 2014; Schaette et al., 2011). The underlying pathophysiological basis of these clinical symptoms have been attributed to damage to the synaptic connections between the inner hair cells and the spiral ganglion axons (Kujawa et al., 2009; Kujawa et al., 2015; Liberman et al., 2017; Liberman et al., 2016; Lin et al., 2011), dyssynchrony of auditory afferent synapses (Roux et al., 2006; Starr et al., 2003), and auditory nerve demyelination (Wan et al., 2017). While these observations suggest the role for neural structural pathogenesis in hearing difficulty, other factors that contribute to these changes following LLN exposure are not fully understood.

Cochlear immunity is an important regulator for cochlear homeostasis and diseases, and macrophages are the major executor in the cochlear immune system (Frye et al., 2017; Hirose et al., 2005; Lang et al., 2006; Okano et al., 2008; Sato et al., 2008; Tornabene et al., 2006; Yang et al., 2015). Numerous researchers have demonstrated that the cochlear macrophage population surrounding the organ of Corti and cochlear neural regions expands in response to signals from these structures successive to sensory cell damage (Fredelius et al., 1990; Frye et al., 2017; Hirose et al., 2005; Ladrech et al., 2007; Sato et al., 2010; Tornabene et al., 2006; Wakabayashi et al., 2010; Yang et al., 2015). These macrophages comprise primarily the infiltrated macrophage precursor cells that transform into mature macrophages in the cochlea. They display pro-inflammatory phenotypes such as increased expression of inflammatory molecules (Yang et al., 2015). In addition to acute cochlear damage, our recent study revealed that chronic low-grade cochlear stress due to age-related and genetic sensory cell degeneration is capable of activating cochlear macrophages (Frye et al., 2017; Zhang et al., 2017). Unlike in the event of acute damage, chronic stress provokes only mild infiltration of monocytes and the major macrophage activity involves mature tissue macrophages. While the precise role of macrophage activities is not clear, these cells have been linked to the generation of local inflammation, the clearance of dead sensory cells (Fredelius, 1988; Fredelius et al., 1990; Hirose et al., 2017) and antigen presentation (Yang et al., 2015). Disruption of macrophage function appears to generate mixed outcomes. For

example, interference of fractalkine signaling has been shown to reduce macrophage recruitment and compromise the survival of cochlear ganglion neurons (Kaur et al., 2015). In contrast, blockage of macrophage infiltration by systemic depletion of macrophages and monocytes alleviates noise-induced hearing dysfunction and sensory cell loss (Mizushima et al., 2017). While the activities of mononuclear phagocytes resultant of acute high-level sensory cell damage have been well documented, cochlear immune cell responses to a low-level stress that does not cause sensory cell death remains elusive.

The current study was designed to examine the morphological and molecular changes of cochlear macrophages in ears that have sustained exposure to LLN. Here, we present evidence of an immune activation following exposure to an intermittent noise at 95 dB SPL that produces only a temporary threshold shift (TTS) without the loss of sensory cells. We reveal that LLN exposure increases the macrophage population in cochlear regions adjacent to sensory cells and the peripheral fibers of spiral ganglion neurons. Moreover, LLN stress causes cochlear macrophages to adopt an activated phenotype and increases the macrophage expression of ICAM-1 and CCL2 in the cochlear region that sustained the acoustic stress. However, macrophages display reduced phagocytic activity after LLN stress. Noticeably, the activated phenotype of macrophages, while recovering partially, persists for at least two months after noise exposure has ceased. Together, these observations clearly implicate cochlear macrophages in cochlear responses to LLN.

2 Experimental Procedures

2.1 Subjects

Male and female CBA/CaJ mice aged 1–3 months were utilized in this investigation. Animals were housed at the University at Buffalo's Laboratory Animal Facility employing a 12-hour lights on and 12-hour lights off (8 AM to 8 PM) light cycle. Procedures involving the use and care of the animal subjects were approved by the Institutional Animal Care and Use Committee of the State University of New York at Buffalo.

2.2 Auditory brainstem responses (ABR)

Auditory brainstem response (ABR) measurements were conducted to assess auditory function using a method previously described in detail (Hu et al., 2012). Briefly, an animal was anesthetized with an intraperitoneal injection of a mixture of ketamine (87 mg/kg) and xylazine (3 mg/kg). Body temperature was maintained at 37.5 °C with a warming blanket (Homeothermic Blanket Control Unit; Harvard Apparatus). Stainless-steel needle electrodes were placed subdermally over the vertex (noninverting input) and posterior to the stimulated and nonstimulated ears (inverting input and ground) of the animal. Elicitation of the ABRs was accomplished with tone bursts at 4, 8, 16, and 32 kHz (0.5 ms rise/fall Blackman ramp, 1 ms duration, alternating phase) at the rate of 21/s. The tone-bursts were generated digitally (SigGen; TDT) using a digital-to-analog converter (100 kHz sampling rate; RP2.1; TDT) and fed to a programmable attenuator (PA5; TDT), an amplifier (SA1; TDT), and a closed-field loudspeaker (CF1; TDT). Electrode outputs were delivered to a preamplifier/base station (RA4LI and RA4PA/RA16B; TDT). Responses were filtered (100–3000 Hz), amplified, and averaged using TDT hardware and software. These responses were then

stored and displayed on a computer. The ABR threshold was defined as the lowest intensity at which an ABR wave I was reliably detectable.

2.3 Noise exposure

Two noise exposure levels were employed: a lower level noise (LLN) at 95 dB SPL and a traumatic noise at 120 dB SPL (sound pressure level, re: 20 μPa). For both experimental conditions the sound intensity was calibrated using a sound level meter (LD-PCB, model 800 B, APCB Piezotronics Div., Larson Davis, Depew, NY, USA) with a condenser microphone (Larson and Davis, LDL 2559, Depew, NY, USA) that was placed at the position of the animal's head in the sound field.

2.3.1 95 dB SPL LLN—The noise signal was generated using Adobe Audition PC-based software (Adobe Systems, San Jose, CA, USA). The signal was routed through an attenuator and power amplifier (L4Z4002, Technical Pro, Edison, NJ, USA) to a low-leakage loudspeaker (FT17H, Fostex, Agoura hills, CA, USA) positioned immediately above each animal holding cage. A continuous noise (8–16 kHz) at 95 dB SPL for 8 hours on and then 16 hours off each day for either 7 or 15 days was used to induce a low-level noise stress to the cochlea. This level of noise exposure was selected because it has been demonstrated to induce temporary threshold shifts and functional changes to the cochlea without resulting in substantial sensory cell death (Furman et al., 2013; Kujawa et al., 2009; Lin et al., 2011). Therefore, this noise exposure paradigm allowed us to evaluate the cochlear immune response to LLN. An additional reason we chose to use this LLN paradigm was to provide a TTS model of chronic noise exposure that correlates well with human noise exposure in an occupational work environment—8 hours of exposure followed by 16 hours of recovery time. During noise exposure, the mice were housed in holding cages with free access to food and water. When the noise was not provided, the animals were housed in the same cages in the same room to prevent stress caused by the frequent change in the residential environment.

2.3.2 120 dB SPL traumatic noise—A broadband noise (1–7 kHz) at 120 dB SPL for 1 hour was used to traumatize the cochlea and to provide the context of a positive control for comparison with our LLN exposure. This level of noise exposure was selected because it causes permanent hearing loss and a substantial degree of sensory cell death (Cai et al., 2014), allowing for the determination of the cochlear immune response to traumatic noise. The noise signal was generated using a Real-Time signal processor (RP2.1, Tucker Davis Technologies, TDT, Alachua, FL, USA). The signal was routed through an attenuator (PA5 TDT, Alachua, FL, USA) and a power amplifier (Crown XLS 202, Harman International Company, Elkhart, IN, USA) to a loudspeaker (NSD2005-8, Eminence, Eminence, KY, USA) positioned above the animal's head. The mice were individually exposed to the noise in a holding cage.

2.4 Cochlear tissue collection

Cochlear tissues were harvested following different experimental paradigms. Animals were euthanized by CO_2 asphyxiation and subsequently decapitated. The cochleae were quickly removed from the skull. For immunostaining of cochlear immune cells, the cochleae were

fixed with either 10% buffered formalin or 4% paraformaldehyde for 1 day. The cochleae were decalcified with 10% Ethylenediaminetetraacetic acid at 4 °C for 1 day and were then dissected in 10 mM phosphate-buffered saline (PBS) to collect the whole-mounts of sensory epithelia containing the basilar membrane, osseous spiral lamina and a lower portion of the lateral wall for subsequent analyses. A portion of the bony shells of the cochleae were also collected for assessing macrophages on the luminal surface of the scala tympani. For animals in the experimental groups (i.e., those subjects that underwent noise exposure), cochlear tissue collection commenced at either 24 hours or 2 months post cessation of noise.

2.5 Determination of sensory cell damage

The assessment of sensory cell damage has been previously reported by our lab (Yang et al., 2015). Tissue collection from animals undergoing noise exposure was completed 24 hours post noise cessation. The pattern of sensory cell damage was determined by quantifying the number of missing inner hair cells (IHC) and outer hair cells (OHC) along the sensory epithelium based on the condition of their cuticular plates and nuclei. For assessment of hair cell cuticular plates, the sensory epithelium surface preparations were incubated with a staining solution containing Alexa Fluor 488 or 568 phalloidin (1:100; Applied Biosystems, Foster City, CA USA) in 10 mM PBS at room temperature in the dark for 30 minutes. For assessment of hair cell nuclei, the tissues were stained with TO-PRO®-3 (1:1,000 1 μM in PBS) a carbocyanine monomer nucleic acid stain, for 30 minutes or 4′,6-Diamidine-2′-phenylindole dihydrochloride (DAPI) (1 μg/ml in PBS) for 10 minutes. After the staining, the tissue was mounted on a slide.

2.6 Immunohistochemistry for immune cell analysis

Immunolabeling of CD45 protein, a pan-leukocyte marker, was used to visualize immune cells. Macrophages were identified based on their expression of ionized calcium-binding adapter molecule 1 (Iba1), a macrophage-specific calcium binding protein that has been used in previous studies for identifying macrophages in the cochlea (Hirose et al., 2005; Okano et al., 2008) and the central nervous system (Ajami et al., 2011). Macrophage precursor cells were identified by their strong expression of lymphocyte antigen 6 complex (Ly6C), a macrophage precursor/monocyte-specific marker (Rose et al., 2012) in combination with relatively weak Iba1 expression. Macrophage and monocyte identity was enhanced by morphological analysis. The overall inflammatory and functional state of macrophage precursor cells and macrophages was further investigated by examining the expression pattern of C-C motif chemokine ligand 2 (CCL2; also known as monocyte chemoattractant protein-1) and the cell surface glycoprotein intercellular adhesion molecule 1 (ICAM-1).

After dissection, whole-mount preparations were treated with 0.5% Triton X-100 to permeabilize the cells for 30 min at room temperature, and then with 10% donkey or goat serum albumin in PBS (pH 7.4) for 1 hour at room temperature. The tissues were subsequently incubated overnight at 4 °C with one or two selected primary antibodies. After incubation with primary antibodies, the tissues were rinsed 3 times in PBS and incubated in the dark with one or two secondary antibodies for 2 hours at room temperature. A comprehensive list of surface markers for these experiments includes: goat anti-CD45 polyclonal antibody, 1:100, AF114, RD Inc., Minneapolis, MN, USA; rabbit anti-Iba1

monoclonal antibody, 1:200, ab178846, Abcam Inc., Cambridge, MA, USA; Ly6C antibody (G-3) mouse monoclonal IgG, 1:100, sc-271811, Santa Cruz Biotechnology Inc., Dallas, TX, USA; rabbit anti-MCP1/CCL2 polyclonal antibody, 1:100, ab25124, Abcam Inc., Cambridge, MA, USA; ICAM-1 antibody (G-5) mouse monoclonal IgG, 1:100, sc-8439, Santa Cruz Biotechnology Inc., Dallas, TX, USA; Alexa Fluor® 488, 555, 568 or 594 donkey anti-goat, anti-rat, anti-rabbit or anti-mouse.

The specificity of the primary antibodies used in this study was confirmed in our previous studies. Briefly, Western blotting of lysates from spleen and lymph node tissues was used to confirm the molecular weights of the proteins targeted by the CD45 antibody (Yang et al., 2015). The Iba1 antibody has been used for identification of macrophages in our previous study examining cochlear tissue macrophages during postnatal development (Dong et al., 2018) and for identification of macrophages/microglia reported in a recent publication (Wang et al., 2017). To prevent false positive identifications due to non-specific labeling of the secondary antibodies, certain samples were incubated with only the secondary antibodies, and no clear fluorescence was observed.

2.7 Macrophage phagocytosis

The phagocytic activity of macrophages under both naive conditions and following noise exposure was evaluated using pHrodo® zymosan bioparticles® conjugate (P35365, Invitrogen, Carlsbad, CA, USA). This pHrodo® dye allows for observation of the degree of phagocytic activity because the fluorescence of the dye is only activated upon ingestion of the zymosan bioparticles by live cells and the exposure of these particles to an increase in pH within the acidic phagocytic vacuoles. Due to the substantially lower extracellular pH, there is a complete lack of bioparticle fluorescence outside the cell bodies. Specifically, animals were euthanized as previously described. The cochleae were quickly removed from the skull and dissected in live cell imaging solution (A14291DJ, Invitrogen, Carlsbad, CA, USA). After the cochlear labyrinth was opened, the sensory epithelia, the modiolus, and the lateral wall were removed to expose the macrophages on the lateral inner surface of the scala tympani of the first cochlear turn. The tissues were then incubated with the pHrodo® zymosan bioparticles® conjugate for 90 minutes at 37 °C and then rinsed 3 times in live cell imaging solution. The tissues were then fixed in 10% buffered formalin for 4 hours, and then decalcified with EDTA at 4 °C for 1 day. Subsequently, the tissues were collected and stained with the antibody against CD45 and an appropriate secondary antibody to visualize immune cells. The tissue was then mounted on a slide containing an antifade mounting medium.

2.8 Tissue observation and image acquisition

The tissues were examined using an epifluorescence illumination microscope (Z6 APO apochromatic zoom system) equipped with a digital camera (DFC3000 G microscope camera) controlled by Leica Application Suite V4 PC-based software (Leica Microsystems, Buffalo Grove, IL, USA). The entire length of the sensory epithelium and immediately surrounding cochlear tissues were photographed. To observe detailed structural changes, certain samples were further examined and photographed using a confocal microscope (LSM510 multichannel laser scanning confocal image system) with associated ZEN Blue

2012 image processing software (Zeiss, Thornwood, NY, USA) utilizing a methodology previously reported (Cai et al., 2014). For macrophage quantification and morphological analysis, the collected images were processed to improve the clarity of cells. Specifically, we used the functions of image adjustment offered in Adobe Photoshop CS6 (version 13.0.1, Adobe Systems, San Jose, CA, USA) to enhance image contrast.

2.9 Quantitative analysis of macrophage morphology and distribution

Macrophages and macrophage precursor cells were identified based on their differential expression of CD45, Iba1 and Ly6C in addition to their shapes and sizes. Macrophages are larger than other types of leukocytes and have unique shapes including dendritic, amoeboid, curvilinear shapes, or an irregular shape with projections. To determine the distribution, we examined cells of interest that had been positively stained with known specific surface markers (either pan-leukocyte marker CD45, macrophage-specific marker Iba1, or macrophage precursor/monocyte marker Ly6C). Positive cells were identified and distinguished from surrounding tissue by their ability to exhibit strong staining patterns in relation to adjacent cells.

Osseous spiral lamina macrophages, basilar membrane macrophages (BM-macrophages) and luminal surface scala tympani macrophages, each identified as a subset of the cochlear macrophage population, were distinguished from neighboring macrophages (e.g., lateral wall macrophages) using the following methods. Bright-field illumination was employed when observing cells under epifluorescence illumination microscopy. This provided clear visual distinction between cochlear partitions: osseous spiral lamina, basilar membrane and surrounding cochlear tissues (e.g., lateral wall). During confocal microscopy, the application of differential interference contrast (DIC) provided clear visualization of tissue orientation, allowing for easy identification of basilar membrane and osseous spiral lamina tissues. Only macrophages residing within a particular cochlear partition were included in the macrophage distribution analysis for that delimited tissue region.

2.9.1 Analyses of basilar membrane macrophages—Macrophage phenotype and distribution was evaluated and described per the following criteria. *General morphology*: a description of immune cell morphology was conducted: e.g., dendritic, amoeboid, networked-curvilinear or small round to teardrop shaped cells. *Cell Size*: measurement of cell size was achieved using Adobe Photoshop to trace cell membrane boundaries. The area contained within each outlined cell was calculated and employed as a metric of cytoplasmic cell area. For each tissue specimen, the area of ten typical cells in the apical portion (0–40% distance from the apical extreme) and ten typical cells in the basal portion (60–100% from the apical extreme) was acquired. These ten cells from each anatomic site were then averaged to provide a single representative number for the apical and basal sections of the basilar membrane for each individual cochlea. *Cell Circularity*: The degree of circularity of individual macrophages was employed to assess gross morphological changes in cellular morphology both under steady-state conditions and subsequent to noise exposure. Specifically, this measure was utilized to reveal to degree to which individual cells demonstrated the following general shapes: dendritic, networked-curvilinear, or amoeboid. Calculation of cellular circularity was acquired in the same procedural step as the acquisition

of cell size using a methodology previously reported (Agley et al., 2012). Adobe Photoshop was used to trace cell membrane boundaries. The *record observations* function provides a measure of circularity with 1.00 indicating a perfect circle. This calculation is derived from $4\pi(\text{area}/\text{perimeter}^2)$. Distribution macrophage-grams were generated using a technique described in our previous publication (Frye et al., 2017). Briefly, the number of cells present per 5% (300 μm) of the total length of the basilar membrane (approximating 6000 μm) was quantified. The mean for these counts was then computed to produce an average value per unit length from the apical extreme to the basal terminus. Group means were acquired by averaging cell counts per unit across specimens for each experimental group.

2.9.2 Analyses of macrophages among the neural tissue of the osseous spiral lamina—Distribution analyses for macrophages residing among the neural tissue of the osseous spiral lamina was performed by quantifying the number of cells present in a sample of 0.1 mm^2 in each of the three anatomical cochlear turns (apical, middle, basal) per specimen. The mean for these counts was then computed to produce an average value per unit area in each cochlea. Group means were acquired by averaging cell counts per unit area across specimens for each group.

2.10 Real-time quantitative polymerase chain reaction (RT-qPCR)

RT-qPCR was performed to determine the transcriptional expression of the following genes: CD14, CCL2, SOD1, TNF-α, IL-1β, Il6, CD86, CCL7, H2A-a, and IL-10. Tissue from the organ of Corti and the lateral wall/basilar membrane were used for analysis. The organ of Corti tissue contains sensory cells (inner hair cells and outer hair cells) and adjacent supporting cells (Deiters cells, pillar cells, Hensen cells, inner phalangeal cells and inner border cells). The lateral wall/basilar membrane tissue contains the mesothelial cells, the basement membrane, immune cells associated with the basilar membrane, cells of Claudius, cells of Boettcher, and all the cells in the stria vascularis and the spiral ligament.

After the animals were euthanized, the cochlea was quickly removed and placed in ice-cold Dulbecco's phosphate buffered saline (PBS, GIBCO, Life Technologies, Grand Island, NY, USA). The bony shell facing the middle ear cavity was quickly removed to expose the cochlear structure. The modiolus of the cochlea was removed, but the lateral wall and the sensory epithelia remained intact. Then, the tissue was placed in RNAlater solution (Qiagen, Valencia, CA, USA) to collect target tissues using techniques described in our previous publications (Cai et al., 2014; Yang et al., 2015). The isolated tissues were transferred to a small dish containing fresh RNAlater solution to wash out tissue debris from the surface of the samples. Then, the tissues were transferred to an RNase-free PCR tube and stored at −80 °C until the analysis of gene expression. The organ of Corti and the lateral wall/basilar membrane tissue from one cochlea was used to generate one sample. There were four biological replicates for each experimental condition (naive control and LLN).

Total RNAs were extracted from the collected tissues using the RNeasy Plus Micro Kit (Qiagen GmbH, Hilden, Germany) and were reverse transcribed using a high capacity cDNA reverse transcription kit (SuperScript™ VILO™ MasterMix, Invitrogen, Carlsbad, CA, USA). RT-qPCR was performed on a CFXConnect Real-Time PCR detection system (Bio-

Rad, Hercules, CA, USA). The transcriptional expression levels of target genes were examined using pre-developed TaqMan gene expression primer/probe assays (Applied Biosystems, Foster City, CA, USA). Pre-developed GABA and Rpl13a gene expression assays (Applied Biosystems) were used as endogenous controls. Analysis of relative gene expression data between sample groups was completed with a standard $2^{-\Delta\Delta Ct}$ method previously reported (Livak et al., 2001).

2.11 Data analyses

Statistical analyses were performed using OriginPro 2017 (OriginLab, Northampton, MA, USA) or SigmaPlot (version 10.0.1.25, San Jose, CA, USA). Group means were statistically compared with either a one- or two-tailed Student's *t* test or a one-way or two-way ANOVA (see Results section for details). An α-level of 0.05 was chosen to denote significance for all statistical tests.

3 Results

3.1 Exposure to an intermittent noise at 95 dB SPL for 2 weeks causes a temporary threshold shift without sensory cell loss

A fundamental aspect of our experiment was to create an experimental condition that exerts a temporal impact on cochlear function, but does not cause sensory cell death. To examine LLN-induced cochlear macrophage activity in the context of changes in hearing sensitivity, we measured ABR thresholds before and at various time points after noise exposure. As compared with the pre-noise thresholds, subjects demonstrated significantly elevated thresholds of 11 ± 3 dB at 4 kHz, 14 ± 3 dB at 8 kHz, 16 ± 4 dB at 16 KHz and 16 ± 3 at 32 kHz following 7 days of LLN exposure. Further elevation of thresholds was observed in subjects exposed to 15 days of LLN with a mean shift of 16 ± 4 dB at 4 kHz, 25 ± 3 dB at 8 kHz, 26 ± 3 dB at 16 kHz and 24 ± 4 dB at 32 kHz. These changes in thresholds are statistically significant (Fig. 1A; Two-way ANOVA, $F(3, 9) = 152$, $P < 0.001$; Holm-Sidak post-hoc method comparisons, Naive vs. 7d LLN, $P < 0.001$; Naive vs. 15d LLN, $P < 0.001$; 7d LLN vs. 15d LLN, $P < 0.001$). Thus, with the prolongation of exposure to LLN (from 7 to 15 days), the degree of threshold shifts further increased suggesting accumulation of functional impacts.

In order to elucidate whether the increase in thresholds was temporary or permanent, ABR measurement was repeated 20 days following noise cessation. By this time point ABR thresholds had returned to the pre-noise level (Fig. 1A; Two-way ANOVA, $F(3, 9) = 152$, $P > 0.05$) indicating that the elevated thresholds measured immediately after the 15-day exposure were TTS. Though previous studies using noises with a similar intensity level, but shorter duration, showed the recovery of thresholds (Furman et al., 2013; Lin et al., 2011), to the best of our knowledge, this is the first study to provide functional assessment data using an extended (7 to 15 day) intermittent 95 dB SPL noise exposure. Together, these functional analyses reveal that our noise exposure paradigm results in only a TTS.

Next, we determined whether the LLN was able to cause sensory cell death using either Alexa Fluor™ 488 phalloidin for f-actin in the cuticular plates of hair cells or DAPI or TO-

PRO®-3 for hair cell nuclei. Loss of Alexa 488 fluorescence in cuticular plates or DAPI/TO-PRO®-3 fluorescence in nuclei is indicative of sensory cell loss. We found no significant increase in the number of missing sensory cells in animals exposed to LLN for either 7 days (0.47% ± 0.14 missing or damaged cells) or 15 days (0.68% ± 0.17) compared to naive controls (0.33% ± 0.21) (Fig. 1; One-way ANOVA, F (3, 17) = 339.671, $P > 0.05$; Tukey post-hoc: LLN 15d vs. Naive, $q = 0.961$, P = 0.904; LLN 15d vs. LLN 7d, $q = 0.552$, $P = 0.979$; LLN 7d vs. Naive, $q = 0.379$, $P = 0.993$). Together, these functional analyses reveal that the LLN used in the current investigation is safe for sensory cell viability.

3.2 Macrophages in the cochlear regions adjacent to sensory cells and neural tissues

We sought to focus on macrophages because these cells are the primary immune cell population in the cochlea (Hirose et al., 2005; Okano et al., 2008) comprising approximately 80% of hematopoietic cells in cochlear tissues (Matern et al., 2017). Moreover, these cells have been demonstrated to be the principal immune cell type activated in the event of cochlear stress and pathogenesis (Frye et al., 2017; Hirose et al., 2005; Lang et al., 2006; Okano et al., 2008; Sato et al., 2008; Tornabene et al., 2006; Yang et al., 2015). In the current study, macrophage identity was defined by their expression of Iba1, a known macrophage-specific protein marker (Ajami et al., 2011) that has been used in cochlear macrophage identification (Hirose et al., 2005; Okano et al., 2008). Our pilot observation showed that Iba1 immunoreactivity correlated well with the immunoreactivity of F4/80, another macrophage marker that has been used in our previous studies (Frye et al., 2017; Yang et al., 2015). Iba1 was selected for macrophage identification in the current study because its immunoreactivity is much stronger than the immunoreactivity of F4/80 in macrophages of cochlear neural regions.

Macrophages have been identified in several cochlear partitions (Hirose et al., 2005; Lang et al., 2006; Sato et al., 2008; Shi, 2010). Here, we focused on two anatomic sites. The first is the neural region within the osseous spiral lamina where macrophages reside among the peripheral bundles of ganglion neurons (Fig. 2). We selected this region because LLN is known to exert adverse effects on spiral ganglion homeostasis (Furman et al., 2013; Kujawa et al., 2009; Lin et al., 2011). Under steady-state conditions, osseous spiral lamina macrophages present with a branched, dendritic morphology as revealed by CD45 and Iba1 immunolabeling (Fig. 3A–C). They are oriented radially toward the lateral edge of the osseous spiral lamina. Moreover, osseous spiral lamina macrophages presented with similar morphology across the apical, middle and basal cochlear portions.

We also observed macrophages in the scala tympani cavity immediately beneath the basilar membrane, and these cells are termed BM-macrophages (Fig. 2). We chose to examine these macrophages because 1) they are in closest anatomic proximity to outer hair cells, the most vulnerable cells to acoustic injury in the cochlea, and 2) these macrophages are readily able to respond and adapt to chronic low-grade cochlear stresses exerted on sensory cells (Frye et al., 2017). Under resting conditions, an apical-to-basal gradient in BM-macrophage morphology was observed. Highly ramified, dendritic-shaped macrophages dominated apical regions (approximately 0–40% from the apex), and this finding is consistent with our previous observations in C57BL/6J mice (Frye et al., 2017; Yang et al., 2015). However,

BM-macrophage morphology in the middle and basal turns of the basilar membrane is notably peculiar. They appeared as a long, thin curvilinear network of cells that stretch along the natural curve of the basilar membrane (Fig. 3D–F).

Macrophages extant on the luminal surface of the scala tympani cavity were also identified and described (Fig. 2). Under resting conditions, these cells are sporadically located and vary in morphology from more highly ramified dendritic-like shapes to more rounded amoeboid phenotypes (Fig. 3G–I).

To further confirm our identity of macrophages, we used immunohistochemistry to stain the bone marrow in the bony shell of the cochlea. Many small, less-differentiated leukocytes expressed strong CD45 immunoreactivity (Fig. 3J). However, Iba1 immunoreactivity was expressed only in well-differentiated macrophages and not in small, round CD45-positive cells (Fig. 3K–L). The finding of strong Iba1 expression in mature mononuclear phagocytes is consistent with previous findings (Ajami et al., 2011). Together, these observations revealed site-dependent morphologies of cochlear macrophages under resting conditions.

3.3 Lower-level noise increases the number of macrophages in the cochlear regions adjacent to sensory cells and neural tissues

Exposure to a high-level noise is known to cause accumulation of inflammatory cells in the cochlea, and these inflammatory cells are thought to come from circulating monocytes in response to sensory cell damage (Hirose et al., 2005; Tornabene et al., 2006; Wakabayashi et al., 2010; Yang et al., 2015). Here, we wanted to know whether exposure to a LLN that does not cause sensory cell death is able to increase the macrophage number in the cochlea. We first examined macrophages in the neural tissue in the osseous spiral lamina. These immune cells are located inside the bony shell of the spiral lamina and are distributed among the neural fibers of ganglion neurons. This cochlear region was selected because macrophages are abundant in this tissue under resting conditions and because pathological changes in the synaptic region of the spiral ganglia have been found following LLN exposure (Kujawa et al., 2009; Kujawa et al., 2015). Changes in the macrophages residing among the neural tissue of the osseous spiral lamina were evaluated as a function of the duration of LLN stress. A tissue area of 0.1 mm^2 was used to survey the number of neural tissue macrophages of each sampled cochlea. Following noise exposure, the number of macrophages in the osseous spiral lamina increased (Fig. 4). While the number of total osseous spiral lamina macrophages increased in cochleae exposed to LLN for 7 days (35 ± 5) compared to naive cochleae (30 ± 5), this increase did not reach significance until 15 days of LLN stress (38 ± 6) (Fig. 4C; One-way ANOVA; $F = 24.95$; df = 2; $P < 0.001$; Tukey test: Naive vs. 7d, $P > 0.05$; Naive vs. 15d, $P < 0.01$; 7d vs. 15d, $P > 0.05$). This observation suggests that a prolonged exposure is able to increase the macrophage number in the neural region of the cochlea.

Next, we examined BM-macrophages because these cells are the closest immune cells to cochlear outer hair cells. We first quantified the total number of BM-macrophages and compared the numbers between the naive and LLN-exposed animals. As compared with the number of BM-macrophages in naive cochleae (114 ± 11), the number of BM-macrophages increased in ears stressed with LLN for both 7 days (151 ± 6) and 15 days (145 ± 4), and

these changes are statistically significant (Fig. 5A; One-way ANOVA, $F(2, 10) = 28.434$, $P < 0.001$; Tukey post-hoc all pairwise multiple comparison, 7d vs. Naive, $q = 9.768$, $P < 0.001$; 15d vs. Naive, $q = 8.175$, $P < 0.001$; 7d vs. 15d, $q = 1.511$, $P > 0.05$.) However, no significant difference was observed between the 7-day and the 15-day group, suggesting no further increase in macrophage number as the noise exposure prolonged from 7 days to 15 days.

Further spatial analysis revealed a site-dependent increase in BM-macrophage numbers (Fig. 5B). Scrutiny of the apical section of the basilar membrane (approximately 0–40% from the apex) revealed no significant difference among groups (Fig. 5C; One-way ANOVA, $F(2, 10) = 25.615$, $P > 0.05$). In contrast, the middle and basal portions of the basilar membrane (40–90% from the apex; see the gray shaded area in Fig. 5B) exhibited an increase in the total number of macrophages after LLN stress. Specifically, the average number of BM-macrophages increased from 74 ± 10 cells observed for the naive group to 108 ± 5 for the 7-day group, and then maintained this increased level (104 ± 5) for the 15 day group (Fig. 5D; One-way ANOVA, $F(2, 10) = 28.434$, $P < 0.001$; Tukey post-hoc all pairwise multiple comparison, 7d vs. Naive, $q = 9.654$, $P < 0.001$; 15d vs. Naive, $q = 8.512$, $P < 0.001$; 7d vs. 15d, $q = 1.084$, $P > 0.05$). This region of macrophage augmentation is consistent with the site of the sensory epithelium corresponding to the frequency of the LLN (8–16 kHz) (Spongr et al., 1997; Willott et al., 2004; Willott et al., 2005). Taken together, these data suggest that LLN stress increases the macrophage population in the cochlear regions adjacent to sensory cells and their neural innervation.

3.4 Infiltrated macrophages in the cochlea after LLN

The finding of the increase in the number of cochlear macrophages suggests the infiltration of circulating monocyte-lineage cells into the cochlea, an immune stress response that has been reported following traumatic noise insult (Hirose et al., 2005; Tornabene et al., 2006; Wakabayashi et al., 2010; Yang et al., 2015). We wanted to know how monocyte-lineage macrophage precursor cells transform during prolongation of LLN. We selected macrophages on the surface of the basilar membrane for this analysis not only because of their close proximity to sensory cells, but also because of the aqueous environment that the cells face, which allows them to adopt a natural shape without significant physical constraints imposed by surrounding cells. This stands in contrast with the macrophages that are embedded within tissues. We identified monocyte-lineage macrophage precursors that were infiltrated as the result of LLN based on their expression of Ly6C (Fig. 6A–B), a protein marker for blood-derived monocytes (Rose et al., 2012) that is associated with inflammatory activity (Rose et al., 2012; Swirski et al., 2009) as well as their morphology—a small and round shape, which differs substantially from tissue macrophages that had a larger body size. We first examined the number of small round $Ly6C^{high}$ cells in the 7-day LLN group. While very few of these cells were present (2 ± 2 cells), a significant increase in the number of these $Ly6C^{high}$ cells was found in cochleae exposed to LLN for 7 days (32 ± 2) (Fig. 6C; One-way ANOVA, $F(2, 10) = 187.409$, $P < 0.001$; Tukey post-hoc all pairwise multiple comparison, 7d vs. Naive, $q = 24.855$, $P < 0.001$). Noticeably, the number of these cells closely matches the number of increased cells along the middle and basal portion of the basilar membrane described in the previous section. Specifically, the total

number of macrophages beneath the basilar membrane increased from 74 ± 9 cells in the naive ears to 108 ± 5 cells in the LLN-stressed ears—an average increase of 34 total cells. This number corresponds to the increase in the number of Ly6C^{high} cells identified at this time point (an average of 30). Further analysis revealed that the Ly6C^{high} cells were confined primarily to the middle and the basal portions of the basilar membrane (see the gray shaded area in Fig. 6D). Again, this distribution is consistent with the distribution of total macrophages observed at this time point (see Fig. 5B). These observations provide further evidence that small round Ly6C^{high} cells are infiltrated monocyte-lineage macrophage precursors.

We then examined the small round Ly6C^{high} cells in the 15-day LLN group and found a significant increase in the number of these cells (29 ± 4) (Fig. 6C; One-way ANOVA, $F(2, 10) = 187.409$, $P < 0.001$; Tukey post-hoc all pairwise multiple comparison, 15d vs. Naive, $q = 21.334$, $P < 0.001$). Again, this increase was confined to the middle and basal portions of the basilar membrane (Fig. 6D) and the level of the increase (average of 27) closely matches the total number of increased macrophages (average of 32) described in the previous section. Noticeably, there was no significant difference in the number of Ly6C^{high} cells between the 7-day group and the 15-day group (Fig. 6C; One-way ANOVA, $F(2, 10) = 187.409$, $P < 0.001$; Tukey post-hoc all pairwise multiple comparison, 7d vs. 15d, $q = 3.340$, $P > 0.05$). These observations suggest that macrophages that infiltrated during the 7-day noise exposure maintained their undifferentiated or less-differentiated phenotypes during the period of additional 8 days of noise exposure.

3.5 Tissue macrophages acquire an activated morphology after exposure to LLN

After analysis of small round Ly6C^{high} cells, we sought to determine the functional state of the macrophages that displayed mature macrophage phenotypes, that is, Iba1-positive cells with a large body size. These cells are likely to be tissue macrophages that already reside in the cochlea under resting conditions. We examined their shape and size because these morphological indexes are an indicator of macrophage activation (Davis et al., 1994; Frye et al., 2017; Raivich et al., 1999; Stence et al., 2001; Young et al., 1969).

For the shape analysis, we measured the circularity of individual macrophages, an indicator of the extent to which a cell shape resembles a circle (with 1.0 representing a perfect circle). As previously stated, macrophages in the apical portion of the basilar membrane displayed a dendritic shape under resting conditions. These cells maintained their ramified morphology after exposure to LLN. Circularity analysis confirms this finding (Fig. 7A; One-way ANOVA, $F(2, 10) = 1.034$, $P > 0.05$).

BM-macrophages in the middle and basal turns of steady-state naive cochleae appear as a network of long, thin curvilinear cells that are aligned with the natural curve of the basilar membrane (arrows, Fig. 7C). However, following LLN stress, cochleae showed few of the curvilinear networked cells typically seen in this cochlear region under steady-state naive conditions. Instead, macrophages acquired a rounded and globular amoeboid shape (single arrows, Fig. 7D)—a morphology associated with an activated immune status (Davis et al., 1994; Frye et al., 2017; Raivich et al., 1999; Stence et al., 2001; Young et al., 1969). In naive cochleae, middle and basal turn macrophages with networked curvilinear morphology

presented with a mean circularity of just 0.08 ± 0.02. However, the globular amoeboid macrophages from this same anatomic site in cochleae stressed for 7 days presented with a circularity of 0.60 ± 0.07 and those stressed for 15 days presented with a circularity of 0.60 ± 0.04. Examination of the degree of circularity of these amoeboid cells revealed a very significant change in their circularity index when compared to naive specimens (Fig. 7B; One-way ANOVA, $F(2, 10) = 188.183$, $P < 0.001$; Tukey post-hoc: 7d vs. Naive, $q = 23.323$, $P < 0.001$; 15d vs. Naive, $q = 23.309$, $P < 0.001$; 7d vs. 15d, $q = 0.014$, $P > 0.05$). This morphological change suggests the activation of tissue macrophages after exposure to LLN.

Next, we measured the cell size. No significant changes in size were observed in apical macrophages after the noise exposure (Fig. 7E; One-way ANOVA, $F(2, 10) = 1.39$, $P > 0.05$). Similarly, no significant changes in the body size were detected for the macrophages in the middle and basal portions of the basilar membrane (Fig. 7F; One-way ANOVA, $F(2, 10) = 1.39$, $P > 0.05$). The finding of the change in the morphology without the change in body size suggests that activated tissue macrophages retract their processes without the change in their body volumes after LLN stress.

3.6 LLN stress induces the expression of ICAM-1 in cochlear macrophages

To determine the functional activation of cochlear macrophages, we examined macrophage expression of the intercellular adhesion molecule 1 (ICAM-1) that has roles in cell differentiation and motility. Expression of ICAM-1 has been experimentally demonstrated to increase in cochleae following acoustic trauma (Tornabene et al., 2006), and previous researchers have shown upregulation of ICAM-1 associated genes following chronic LLN stresses (Tan et al., 2016). Here, we examined the expression of ICAM-1 in cochlear macrophages following 15 days of our LLN paradigm. Immunoreactivity of ICAM-1 under naive steady-state conditions is weak (Fig. 8A–C). In contrast, the immunoreactivity of ICAM-1 was markedly increased on cochlear macrophages chronically stressed with LLN (Fig. 8D–F). Noticeably, small round cells display a higher immunoreactivity than large branched cells. Taken together these data show that the expression of ICAM-1, an important molecule associated with changes in both inner ear immune status (Suzuki et al., 1995; Tan et al., 2016; Tornabene et al., 2006) and the migration of leukocytes to the ear (Shi et al., 2007), is upregulated in cochlear macrophages following LLN stress.

3.7 LLN stress inhibits macrophage phagocytic function

Observed changes in the cochlear macrophage morphology following LLN stress suggests changes in macrophage function. To provide further evidence for changes in macrophage function, we examined macrophage phagocytic activity because this function has been implicated in removing unwanted or damaged tissues from the cochlea under normal and pathological conditions (Fredelius et al., 1990; Hirose et al., 2017; Hu et al., 2018). We used pHrodo® zymosan bioparticles® for assessing phagocytosis of macrophages. This assay allows for determining the level of phagocytic activity because the fluorescence intensity of zymosan bioparticles is correlated to the level of ingested zymosan bioparticles. Macrophages located on the luminal surface of the scala tympani cavity were selected for

observation because these cells were able to access the pHrodo® bioparticles during the *in vitro* staining process.

Naive ears and those stressed with LLN for 15 days were examined using a confocal microscope with identical parameter settings (Fig. 9A–F). We first counted the number of macrophages on the luminal surface of the scala tympani and found no significant difference in the number of macrophages between the naive and LLN-exposed ears (27 ± 6 for the control ears vs. 23 ± 3 for the LLN-stressed ears; Student's t-test, $t(6) = 1.12$, $P > 0.05$; Fig. 9G). Next, we counted the number of macrophages that displayed pHrodo® fluorescent bioparticles within their bodies and then calculated the percentage of pHrodo fluorescence-positive cells over the total macrophages in the examined area. In control cochleae, a larger of proportion of cells displayed the bioparticles (68.3% ± 3.2) when compared to the relatively smaller proportion of macrophages displaying the bioparticles in ears stressed by LLN for 15 days (45.0% ± 7.4), and this difference is statistically significant (Fig. 9H; Student's t-test, $t(6) = 5.79$, $P < 0.001$). We further scrutinized the number of ingested particles by measuring the intensity of pHrodo® fluorescence in all macrophages that presented with bioparticles within their cell bodies. Though some proportion of macrophages in both naive and LLN-stressed ears participated in phagocytosis of pHrodo® bioparticles, those macrophages in naive ears showed far greater pHrodo® fluorescence levels (average gray level of 33.9 ± 7.6) compared to ears that had been exposed to LLN for 15 days (average gray level of 14.5 ± 3.9). This difference is significant (Fig. 9I; Student's t-test, $t(6) = 4.55$, $P < 0.004$), Collectively, these findings suggest that the phagocytic capacity of cochlear macrophages is reduced following LLN stress, which provides another piece of evidence that LLN stress is able to alter cochlear macrophage function.

3.8 Cochlear inflammatory activity following LLN

To determine whether LLN provokes cochlear inflammatory activity, we investigated the transcriptional expression of a group of genes that have been implicated in proinflammatory activity (CCL2, TNF-α, IL-1β, IL6, CCL7), anti-inflammatory activity (SOD1), antigen presentation (CD86, H2-Aa), and other immune functions in the cochlea (CD14) (Cai et al., 2014; Tan et al., 2016; Vethanayagam et al., 2016). Cochlear tissues containing sensory and non-sensory cells were collected from experimental animals exposed to LLN for 15 days (n=4 biological replicates) and naive controls (n=4 biological replicates). In LLN-stressed cochleae, we found downregulation of five immune-related genes (CCL2, TNF-α, IL-1β, SOD1, CD14,) and upregulation of four others (CCL7, IL6, CD86, H2-Aa) as compared to naive controls. However, only the downregulation of the chemokine-chemokine (C–C motif) ligand 2 (CCL2) reached statistical significance (Fig. 10; Student's t-test, $t(6) = 2.90$, $P = 0.027$).

To determine whether the decrease in CCL2 expression occurs in macrophages, we employed immunohistochemistry to define its expression level. We first examined the networked curvilinear BM-macrophages in the control cochleae, and no detectable CCL2 immunoreactivity was detected (Fig. 11A–C). To provide a context for assessing the level of CCL2 upregulation in LLN-stressed macrophages we next surveyed CCL2 immunoreactivity in cochlear macrophages after exposure to a high level of acoustic

overstimulation (120 dB SPL for 1 hour), a paradigm that has been used in our previous study to provoke the inflammatory response to sensory cell degeneration in the cochlea (Yang et al., 2015). In high-level noise traumatized cochleae, the macrophages located immediately beneath the basilar membrane are small and round to teardrop shaped with strong CD45 and CCL2 expression (Fig. 11D). These morphological changes are similar to our previous finding in C57BL/6J mice that sustained the same level of acoustic overstimulation. In these cochleae, strong CCL2 expression was observed in BM-macrophages, particularly in small round macrophages (Fig. 11E–F). We then examined the CCL2 immunoreactivity following LLN stress for 15 days. The macrophages, which possessed a rounded amoeboid shape (Fig. 11G), demonstrated weak CCL2 immunoreactivity (Fig. 11H–I). Further quantitative analysis of CCL2 fluorescence intensity revealed that CCL2 immunoreactivity in the LLN-stressed ears (12.22 ± 1.5) was slightly higher than that in the control ears (1.69 ± 0.5). However, this increased level is significantly lower than that observed in the ears that sustained exposure to high-intensity noise (45.75 ± 11.7) (Fig. 11J; One-way ANOVA, $F(2, 18) = 79.147$, $P < 0.001$; Tukey post-hoc all pairwise multiple comparison, Naive vs. 120 dB, $q = 44.056$, $P < 0.001$; Naive vs. LLN, $q = 4.071$, $P < 0.05$; 120 dB vs. LLN, $q = 12.965$, $P < 0.001$). This observation suggests that activated macrophages following LLN do express the proinflammatory cytokine CCL2, but the expression level is much less than that observed in high-level noise traumatized cochleae.

3.9 Macrophages two months after LLN cessation

Because BM-macrophages beneath the middle and basal portion of the sensory epithelia underwent substantial changes in number and cell shape during LLN stress, we wanted to know whether these changes were reversible after a recovery period. Animals that had first been stressed with LLN for 15 days were subsequently removed from noise and the cochleae were collected 2 months after noise exposure. At this time, hearing sensitivity had recovered (See Fig. 1A). Enumeration of middle and basal BM-macrophages revealed not only a complete recovery, but also a reduction in the number of these cells (58 ± 5) to below the pre-noise level (74 ± 10) despite an initial increase in the number of these cells observed right after the noise (105 ± 5) (Fig. 12D; One-way ANOVA, $F(2, 10) = 28.434$, $P < 0.001$; Tukey post-hoc all pairwise multiple comparison, Right after noise vs. 2 months after noise, $q = 12.682$, $P < 0.001$; Right after noise vs. Pre-noise, $q = 8.854$, $P < 0.001$; Pre-noise vs. 2 months after noise, $q = 4.513$, $P < 0.05$). This suggests a biphasic BM-macrophage response where the early response is an increase in the population of BM-macrophages followed by a reduction of these cells 2 months after noise cessation. Consistent with this finding is that the number of $Ly6C^{high}$ cells returned to the pre-noise level (an average of 2 ± 2 cells).

Further morphological analysis revealed that BM-macrophages no longer possessed the highly amoeboid morphologies observed right after the noise (see Fig. 7D). Though these cells were morphologically distinguishable from the curvilinear networked cells typical of naive pre-noise ears (see Fig. 3D–F), the BM-macrophages in cochleae 2 months after noise began to return to a more branched morphology but with generally shorter processes. Empirical analysis employing the previously described circularity index revealed a much reduced cell circularity 2 months after the noise (0.27 ± 0.08) compared to the circularity of

BM-macrophages right after the noise (0.60 ± 0.04). Yet, these cells were still significantly more amoeboid in shape compared to pre-noise conditions (0.08 ± 0.02) (Fig. 12E; One-way ANOVA, $F(2, 10) = 115.616$, $P < 0.001$; Tukey post-hoc: Right after noise vs. Pre-noise, $q = 21.412$, $P < 0.001$; Right after noise vs. 2 months after noise, $q = 12.983$, $P < 0.001$; 2 months after noise vs. Pre-noise, $q = 7.727$, $P < 0.001$). This observation revealed that the morphological change in BM-macrophages recovers only partially at 2 months after LLN.

4 Discussion

We investigated the effects of LLN on cochlear immune homeostasis, with particular attention paid to changes to the primary immune executor in the inner ear: cochlear macrophages. Specifically, we examined the number, distribution, morphology and functional state of macrophages in addition to molecular changes within the cochlea following extended exposure to LLN. Critically, in this investigation, we employed a noise paradigm that mirrors typical human occupational noise with repeated exposures to 8 hours of LLN that results in a TTS followed by a 16-hour resting time. We reveal five major findings. First, an intermittent LLN that causes only TTS is able to increase the macrophage population in the regions adjacent to sensory cells and the peripheral axons of the spiral ganglia. Second, LLN induces a morphological transition of BM-macrophages (the closest macrophages to sensory cells) to activated phenotypes in the middle and basal portions of the basilar membrane corresponding to the region of the sensory epithelium receiving the maximum mechanical force of the noise (8—16 kHz). Third, exposure to LLN causes a reduction in macrophage phagocytic capacity, an essential function of macrophages for tissue homeostasis. Fourth, protein expression of ICAM-1 and CCL2 is upregulated in cochlear macrophages although changes in transcriptional expression of major proinflammatory genes are not detected in the cochlea. Finally, while the increased number of cochlear macrophages has returned to the pre-noise level, their active morphology only partially recovers 2 months after noise cessation, long after hearing sensitivity has returned to the baseline. Together, these observations suggest that a “hearing sensitivity safe” noise is able to alter the cochlear immune system for an extended period of time.

Previous studies have documented the immune cell responses to cochlear damage induced by exposure to high levels of cochlear stresses including acoustic overstimulation that cause sensory cell degeneration. Here, we investigated the immune impact of a LLN exposure that caused only TTS. Our study documented both similarity and difference in macrophage responses as compared with those induced by exposure to a high-level noise observed in the current study as well as reported in our previous study (Yang et al., 2015). Both high-level noise and LLN result in a rise in the cochlear macrophage population, but as expected the conditions demonstrate a different level of the increase with a greater number of cells observed following high-level noise trauma compared to the relatively fewer number observed subsequent to chronic LLN stress. In both instances, macrophages display an activated morphology, but with different characteristics. LLN-stressed macrophages largely adopt an amoeboid phenotype, while macrophages appear in an irregular shape with many long or short processes in the event of traumatic overstimulation. Additionally, both types of acoustic stress instigate increased expression of inflammatory molecules, but again have different levels of enhancement. While CCL2 expression in both macrophages and other

cochlear tissue is upregulated following traumatic acoustic injury, LLN stress produces only mild CCL2 expression in macrophages. Moreover, in cochleae that sustained a high-level noise exposure, infiltrated cells appear to dominate the inflammatory response. In contrast, cochleae that sustained chronic LLN demonstrate tissue macrophages as the major player of inflammatory activity. These differences are likely to be caused by the difference in the level of inflammatory activities. As shown in several previous studies (Cai et al., 2014; Fujioka et al., 2006; Tornabene et al., 2006; Yang et al., 2016), a high-level noise can cause significant upregulation of inflammatory molecules in the cochlea. Although these studies were performed in a different mouse strain (C57BL/6 or Harlan Sprague-Dawley), high-level noise exposures are likely to produce similar results in our experimental mice (CBA/CaJ) because our study showed a significant increase in macrophage expression of CCL2 after exposure to a high-level noise. In contrast, our current study reveals no detectable upregulation of inflammatory mediators in the cochlear tissue following LLN exposure. Together, these observations suggest that LLN-induced macrophage responses bear many characteristics of high-level noise-induced macrophage responses, but to a lesser extent.

Chronic cochlear stresses such as insidious age-related sensory cell degeneration are capable of activating cochlear macrophages (Frye et al., 2017). The major difference between aging stress and LLN stress is the presence of considerable hair cell death in the former and the absence of substantial hair cell death in the latter. Despite minimal or negligible sensory cell loss in the event of LLN stress, any proinflammatory cochlear response precipitated by the LLN exposure is likely to affect cochlear homeostasis. In some ways, the LLN-induced macrophage response is similar to that caused by chronic cochlear pathogenesis due to aging (Frye et al., 2017) and certain genetic mutations (Zhang et al., 2017). The immune response in both LLN-stressed ears and aging ears involves primarily mature tissue macrophages, and macrophages undergo amoeboid transformation. However, the location and timing of this transformation is distinct in each event. In aging ears, these dynamic changes in morphology are spatially correlated to the stages of sensory cell degeneration (Frye et al., 2017). In contrast, BM-macrophage amoeboid transformation occurs concurrently across a broad length of the sensory epithelium (40–100% from the apex) during LLN-stress. Moreover, in the event of chronic sensory cell degeneration, the amoeboid cells increase in size in regions of the sensory epithelia undergoing active sensory cell pathogenesis (Frye et al., 2017). However, no overall change in cell size occurred in LLN-stressed ears despite a conspicuous transformation of macrophages in the middle and basal regions. This differential pattern of amoeboid activation suggests that a unique immune response is mounted in the event of LLN stress compared to chronic age-related sensory cell degeneration because changes in morphology can modulate the functional state of the macrophage (McWhorter et al., 2013). It should be noted that the difference observed in the current study as compared with those observed in our previous study could also be associated with an animal strain difference (CBA/CaJ used in the current study vs. C57BL/6J used in our previous studies) because macrophages display different morphologies under resting conditions in these two strains.

A compelling finding of the current study is a reduction in macrophage phagocytic capacity following 15 days of our intermittent LLN paradigm. As reported in the results section, we observed a decrease in the phagocytic activity of cochlear macrophages following LLN stress. It is likely that this reduced phagocytic ability is related to the increase in pro-

inflammatory activity in cochlear macrophages because these cells display an increase in CCL2 expression and because an upsurge of pro-inflammatory cytokines has been shown to inhibit macrophage phagocytosis in the central nervous system (Koenigsknecht-Talboo et al., 2005). This local effect of LLN on the cochlear macrophages is consistent with a systemic effect of low-level noise stress on circulating phagocytes. As demonstrated in a previous study, exposure to a chronic intermittent noise (85 dB SPL, 2–20 kHz) caused a reduction in the phagocytic capacity of circulating blood monocytes (Van Raaij et al., 1996). Phagocytosis is an essential function performed by cochlear macrophages for clearance of cellular debris after stress as well as under resting conditions (Fredelius, 1988; Hirose et al., 2017; Hu et al., 2018), and diminished macrophage phagocytic ability may have far-reaching implications for cochlear homeostasis. Cumulatively, these findings suggest chronic LLN stresses alter macrophage functional capacity, and the reduced ability of cochlear macrophages to perform essential functions has the potential to influence damage resolution and the healing process—an important future biological target for remediating inner ear damage (Kalinec et al., 2017). Whether such changes could affect macrophage phagocytic function in future encounters with dead cells due to exposure to subsequent traumatic noise warrants further investigations.

To determine the inflammatory state of the cochlea after LLN, we investigated the transcriptional expression of a group of genes implicated in immune activity. This analysis did not detect augmentation of the overall inflammatory state in the cochlea. This negative finding could be caused by our sample composition that contains both immune cells and non-immune cells. This mixed cellular composition can diminish the test sensitivity for detecting minor changes that occurred in specific cell populations. This could also be the cause of the conflicting finding that a decrease in CCL2 expression was detected in cochlear tissues even though a CCL2 expression increase was found in cochlear macrophages following LLN stress. Nevertheless, our data suggest the overall inflammatory activities of the cochlea are mild as compared with that seen after traumatic noise exposure. Yet, macrophages display activated morphologies following LLN stress. This finding clearly indicates that the cochlear macrophage is a more sensitive internal sensor for changes to cochlear homeostasis than can be provided by a gross assessment of cochlear expression of immune related genes. What is more, it suggests macrophages may be involved in a low level of inflammatory activity following LLN exposure.

Changes in cochlear macrophage activities could affect synapse homeostasis. A lower level of acoustic overstimulation is known to affect cochlear homeostasis and hearing function, including a long-term effect on the amplitude of ABR wave I (Kujawa et al., 2009). Changes to hearing function have been linked to the loss of synapses connecting inner hair cells and their innervations (Kujawa et al., 2006; Kujawa et al., 2009), and macrophages have been found to play an important role in synapse pathophysiology (Amit et al., 2016; Paolicelli et al., 2011; Takano et al., 2014). While our current observation did not find macrophages in the immediate vicinity of inner hair cells, we did notice an increase in the number of macrophages in the osseous spiral lamina following chronic LLN stress. Where these macrophages reside inside in the bony tunnel of the osseous spiral lamina, their processes extend via the habenulae perforata toward the region of inner hair cells. Previous researchers found that dysfunction of macrophage activity potentiates damage to neural components

(Kaur et al., 2015). It is likely that these cells could participate in the immune response to the increased activity in the synapse due to noise overexposures. Though we did not examine ABR amplitudes and synapse conditions in this study, the LLN exposure paradigm we employed is likely to produce a comparable effect on the summed activity of the auditory nerve fibers, and this phenomenon should be investigated in future studies. Further future investigations are warranted in delineating the precise interplay between macrophages and neuronal components of the cochlea. Such undertakings could help shed light on functional modifications within the cochlea and how these changes may relate to hearing difficulties in patients with normal hearing sensitivity.

Acknowledgments

Funding: This work was supported by the National Institute on Deafness and Other Communication Disorders of the National Institutes of Health [R01DC010154 (BHH)] and the American Academy of Audiology Foundation [Research Grant in Hearing and Balance (Mitchell Frye)]. The authors would like to thank Guang-Di Chen and Xiao-Peng Liu for their work in implementing the lower level noise exposure paradigm. We would also like to thank Katelyn Murphy and Megan Nowacki for their assistance in animal subject functional assessments and Carley Cuzzacrea for creating the anatomic schematic of the cochlea.

Abbreviations

BM-macrophages	Basilar membrane macrophages
CCL2	C-C motif chemokine ligand 2
CD45	Cluster of differentiation 45
ICAM-1	Intercellular adhesion molecule 1
Iba1	Ionized calcium-binding adapter molecule 1
Ly6C	Lymphocyte antigen 6 complex
PBS	Phosphate-buffered saline

References

Agley CC, Velloso CP, Lazarus NR, Harridge SDR. An Image Analysis Method for the Precise Selection and Quantitation of. Journal of Histochemistry and Cytochemistry. 2012; 60:428–38. [PubMed: 22511600]

Ajami B, Bennett JL, Krieger C, McNagny KM, Rossi FM. Infiltrating monocytes trigger EAE progression, but do not contribute to the resident microglia pool. Nat Neurosci. 2011; 14:1142–9. [PubMed: 21804537]

Amit I, Winter DR, Jung S. The role of the local environment and epigenetics in shaping macrophage identity and their effect on tissue homeostasis. Nat Immunol. 2016; 17:18–25. [PubMed: 26681458]

Bharadwaj HM, Masud S, Mehraei G, Verhulst S, Shinn-Cunningham BG. Individual differences reveal correlates of hidden hearing deficits. J Neurosci. 2015; 35:2161–72. [PubMed: 25653371]

Cai Q, Vethanayagam RR, Yang S, Bard J, Jamison J, Cartwright D, Dong Y, Hu BH. Molecular profile of cochlear immunity in the resident cells of the organ of Corti. Journal of Neuroinflammation. 2014; 11:173. [PubMed: 25311735]

Davis EJ, Foster TD, Thomas WE. Cellular forms and functions of brain microglia. Brain Res Bull. 1994; 34:73–8. [PubMed: 8193937]

Dong Y, Zhang C, Frye M, Yang W, Ding D, Sharma A, Guo W, Hu BH. Differential fates of tissue macrophages in the cochlea during postnatal development. Hearing Research. 2018; 365:110–126. [PubMed: 29804721]

Fredelius L. Time sequence of degeneration pattern of the organ of Corti after acoustic overstimulation. A transmission electron microscopy study. Acta oto-laryngologica. 1988; 106:373–85. [PubMed: 3207005]

Fredelius L, Rask-Andersen H. The role of macrophages in the disposal of degeneration products within the organ of corti after acoustic overstimulation. Acta oto-laryngologica. 1990; 109:76–82. [PubMed: 2309562]

Frye MD, Yang W, Zhang C, Xiong B, Hu BH. Dynamic activation of basilar membrane macrophages in response to chronic sensory cell degeneration in aging mouse cochleae. Hear Res. 2017; 344:125–134. [PubMed: 27837652]

Fujioka M, Kanzaki S, Okano HJ, Masuda M, Ogawa K, Okano H. Proinflammatory cytokines expression in noise-induced damaged cochlea. Journal of Neuroscience Research. 2006; 83:575–583. [PubMed: 16429448]

Furman AC, Kujawa SG, Liberman MC. Noise-induced cochlear neuropathy is selective for fibers with low spontaneous rates. J Neurophysiol. 2013; 110:577–86. [PubMed: 23596328]

Hamernik RP, Henderson D, Coling D, Slepecky N. The interaction of whole body vibration and impulse noise. J Acoust Soc Am. 1980; 67:928–34. [PubMed: 7358917]

Hamernik RP, Turrentine G, Roberto M, Salvi R, Henderson D. Anatomical correlates of impulse noise-induced mechanical damage in the cochlea. Hearing Research. 1984; 13:229–247. [PubMed: 6735931]

Henderson D, Salvi RJ. Effects on noise exposure on the auditory functions. Scandinavian audiology Supplementum. 1998; 48:63–73. [PubMed: 9505299]

Hickox AE, Liberman MC. Is noise-induced cochlear neuropathy key to the generation of hyperacusis or tinnitus? J Neurophysiol. 2014; 111:552–64. [PubMed: 24198321]

Hirose K, Rutherford MA, Warchol ME. Two cell populations participate in clearance of damaged hair cells from the sensory epithelia of the inner ear. Hear Res. 2017

Hirose K, Discolo CM, Keasler JR, Ransohoff R. Mononuclear phagocytes migrate into the murine cochlea after acoustic trauma. The Journal of Comparative Neurology. 2005; 489:180–194. [PubMed: 15983998]

Hu B. Noise-Induced Structural Damage to the Cochlea. In: Le Prell CG, Henderson D, Fay RR, Popper AN, editorsNoise-Induced Hearing Loss: Scientific Advances. Springer; New York, New York, NY: 2012. 57–86.

Hu BH, Zhang C, Frye MD. Immune cells and non-immune cells with immune function in mammalian cochleae. Hearing Research. 2018; 362:14–24. [PubMed: 29310977]

Hu BH, Guo W, Wang PY, Henderson D, Jiang SC. Intense noise-induced apoptosis in hair cells of guinea pig cochleae. Acta oto-laryngologica. 2000; 120:19–24. [PubMed: 10779180]

Hu BH, Cai Q, Hu Z, Patel M, Bard J, Jamison J, Coling D. Metalloproteinases and Their Associated Genes Contribute to the Functional Integrity and Noise-Induced Damage in the Cochlear Sensory Epithelium. The Journal of Neuroscience. 2012; 32:14927–14941. [PubMed: 23100416]

Kalinec GM, Lomberk G, Urrutia RA, Kalinec F. Resolution of Cochlear Inflammation: Novel Target for Preventing or Ameliorating Drug-, Noise- and Age-related Hearing Loss. Front Cell Neurosci. 2017; 11:192. [PubMed: 28736517]

Kaur T, Zamani D, Tong L, Rubel EW, Ohlemiller KK, Hirose K, Warchol ME. Fractalkine Signaling Regulates Macrophage Recruitment into the Cochlea and Promotes the Survival of Spiral Ganglion Neurons after Selective Hair Cell Lesion. J Neurosci. 2015; 35:15050–61. [PubMed: 26558776]

Koenigsknecht-Talboo J, Landreth GE. Microglial phagocytosis induced by fibrillar beta-amyloid and IgGs are differentially regulated by proinflammatory cytokines. J Neurosci. 2005; 25:8240–9. [PubMed: 16148231]

Kujawa SG, Liberman MC. Acceleration of age-related hearing loss by early noise exposure: evidence of a misspent youth. J Neurosci. 2006; 26:2115–23. [PubMed: 16481444]

Kujawa SG, Liberman MC. Adding insult to injury: cochlear nerve degeneration after “temporary” noise-induced hearing loss. J Neurosci. 2009; 29:14077–85. [PubMed: 19906956]

Kujawa SG, Liberman MC. Synaptopathy in the noise-exposed and aging cochlea: Primary neural degeneration in acquired sensorineural hearing loss. Hear Res. 2015; 330:191–9. [PubMed: 25769437]

Ladrech S, Wang J, Simonneau L, Puel JL, Lenoir M. Macrophage contribution to the response of the rat organ of Corti to amikacin. J Neurosci Res. 2007; 85:1970–9. [PubMed: 17497672]

Lang H, Ebihara Y, Schmiedt RA, Minamiguchi H, Zhou D, Smythe N, Liu L, Ogawa M, Schulte BA. Contribution of bone marrow hematopoietic stem cells to adult mouse inner ear: Mesenchymal cells and fibrocytes. The Journal of Comparative Neurology. 2006; 496:187–201. [PubMed: 16538683]

Liberman MC, Kujawa SG. Hear Res. 2017. Cochlear synaptopathy in acquired sensorineural hearing loss: Manifestations and mechanisms.

Liberman MC, Epstein MJ, Cleveland SS, Wang H, Maison SF. Toward a Differential Diagnosis of Hidden Hearing Loss in Humans. PLoS One. 2016; 11:e0162726. [PubMed: 27618300]

Lin HW, Furman AC, Kujawa SG, Liberman MC. Primary neural degeneration in the Guinea pig cochlea after reversible noise-induced threshold shift. J Assoc Res Otolaryngol. 2011; 12:605–16. [PubMed: 21688060]

Livak KJ, Schmittgen TD. Analysis of relative gene expression data using real-time quantitative PCR and the 2(−Delta Delta C(T)) Method. Methods (San Diego, Calif). 2001; 25:402–8.

Matern M, Vijayakumar S, Margulies Z, Milon B, Song Y, Elkon R, Zhang X, Jones SM, Hertzano R. Gfi1(Cre) mice have early onset progressive hearing loss and induce recombination in numerous inner ear non-hair cells. Scientific reports. 2017; 7:42079. [PubMed: 28181545]

McWhorter FY, Wang T, Nguyen P, Chung T, Liu WF. Modulation of macrophage phenotype by cell shape. Proceedings of the National Academy of Sciences. 2013; 110:17253.

Mizushima Y, Fujimoto C, Kashio A, Kondo K, Yamasoba T. Macrophage recruitment, but not interleukin 1 beta activation, enhances noise-induced hearing damage. Biochem Biophys Res Commun. 2017; 493:894–900. [PubMed: 28951212]

Okano T, Nakagawa T, Kita T, Kada S, Yoshimoto M, Nakahata T, Ito J. Bone marrow-derived cells expressing Iba1 are constitutively present as resident tissue macrophages in the mouse cochlea. Journal of Neuroscience Research. 2008; 86:1758–1767. [PubMed: 18253944]

Paolicelli RC, Bolasco G, Pagani F, Maggi L, Scianni M, Panzanelli P, Giustetto M, Ferreira TA, Guiducci E, Dumas L, Ragozzino D, Gross CT. Synaptic pruning by microglia is necessary for normal brain development. Science. 2011; 333:1456–8. [PubMed: 21778362]

Raivich G, Bohatschek M, Kloss CU, Werner A, Jones LL, Kreutzberg GW. Neuroglial activation repertoire in the injured brain: graded response, molecular mechanisms and cues to physiological function. Brain Res Brain Res Rev. 1999; 30:77–105. [PubMed: 10407127]

Rose S, Misharin A, Perlman H. A novel Ly6C/Ly6G-based strategy to analyze the mouse splenic myeloid compartment. Cytometry Part A: the journal of the International Society for Analytical Cytology. 2012; 81:343–350. [PubMed: 22213571]

Roux I, Safieddine S, Nouvian R, Grati M, Simmler MC, Bahloul A, Perfettini I, Le Gall M, Rostaing P, Hamard G, Triller A, Avan P, Moser T, Petit C. Otoferlin, defective in a human deafness form, is essential for exocytosis at the auditory ribbon synapse. Cell. 2006; 127:277–89. [PubMed: 17055430]

Sato E, Shick HE, Ransohoff RM, Hirose K. Repopulation of cochlear macrophages in murine hematopoietic progenitor cell chimeras: The role of CX3CR1. The Journal of Comparative Neurology. 2008; 506:930–942. [PubMed: 18085589]

Sato E, Shick HE, Ransohoff RM, Hirose K. Expression of fractalkine receptor CX3CR1 on cochlear macrophages influences survival of hair cells following ototoxic injury. J Assoc Res Otolaryngol. 2010; 11:223–34. [PubMed: 19936834]

Saunders JC, Dear SP, Schneider ME. The anatomical consequences of acoustic injury: A review and tutorial. J Acoust Soc Am. 1985; 78:833–60. [PubMed: 4040933]

Schaette R, McAlpine D. Tinnitus with a normal audiogram: physiological evidence for hidden hearing loss and computational model. J Neurosci. 2011; 31:13452–7. [PubMed: 21940438]

Shi X. Resident macrophages in the cochlear blood-labyrinth barrier and their renewal via migration of bone-marrow-derived cells. Cell Tissue Res. 2010; 342:21–30. [PubMed: 20838812]

Shi X, Nuttall AL. Expression of adhesion molecular proteins in the cochlear lateral wall of normal and PARP-1 mutant mice. Hear Res. 2007; 224:1–14. [PubMed: 17184942]

Spongr VP, Flood DG, Frisina RD, Salvi RJ. Quantitative measures of hair cell loss in CBA and C57BL/6 mice throughout their life spans. J Acoust Soc Am. 1997; 101:3546–53. [PubMed: 9193043]

Starr A, Michalewski HJ, Zeng FG, Fujikawa-Brooks S, Linthicum F, Kim CS, Winnier D, Keats B. Pathology and physiology of auditory neuropathy with a novel mutation in the MPZ gene (Tyr145->Ser). Brain: a journal of neurology. 2003; 126:1604–19. [PubMed: 12805115]

Stence N, Waite M, Dailey ME. Dynamics of microglial activation: a confocal time-lapse analysis in hippocampal slices. Glia. 2001; 33:256–66. [PubMed: 11241743]

Sulkowski W, Starzynski Z, Szeszenia-Dabrowska N. Epidemiology of occupational noise-induced hearing loss in Poland throughout 1971--1979. Med Pr. 1981; 32:9–16. [PubMed: 7289864]

Suzuki M, Harris JP. Expression of intercellular adhesion molecule-1 during inner ear inflammation. Ann Otol Rhinol Laryngol. 1995; 104:69–75. [PubMed: 7530436]

Swirski FK, Nahrendorf M, Etzrodt M, Wildgruber M, Cortez-Retamozo V, Panizzi P, Figueiredo JL, Kohler RH, Chudnovskiy A, Waterman P, Aikawa E, Mempel TR, Libby P, Weissleder R, Pittet MJ. Identification of splenic reservoir monocytes and their deployment to inflammatory sites. Science. 2009; 325:612–6. [PubMed: 19644120]

Takano M, Kawabata S, Komaki Y, Shibata S, Hikishima K, Toyama Y, Okano H, Nakamura M. Inflammatory cascades mediate synapse elimination in spinal cord compression. Journal of Neuroinflammation. 2014; 11:40–40. [PubMed: 24589419]

Tan WJ, Thorne PR, Vlajkovic SM. Characterisation of cochlear inflammation in mice following acute and chronic noise exposure. Histochem Cell Biol. 2016; 146:219–30. [PubMed: 27109494]

Taylor W, Pearson J, Mair A, Burns W. STUDY OF NOISE AND HEARING IN JUTE WEAVING. J Acoust Soc Am. 1965; 38:113–20. [PubMed: 14347600]

Tornabene SV, Sato K, Pham L, Billings P, Keithley EM. Immune cell recruitment following acoustic trauma. Hearing Research. 2006; 222:115–124. [PubMed: 17081714]

Van Raaij MT, Oortgiesen M, Timmerman HH, Dobbe CJ, Van Loveren H. Time-dependent differential changes of immune function in rats exposed to chronic intermittent noise. Physiology & behavior. 1996; 60:1527–33. [PubMed: 8946501]

Vethanayagam RR, Yang W, Dong Y, Hu BH. Toll-like receptor 4 modulates the cochlear immune response to acoustic injury. Cell Death Dis. 2016; 7:e2245. [PubMed: 27253409]

Wakabayashi K, Fujioka M, Kanzaki S, Okano HJ, Shibata S, Yamashita D, Masuda M, Mihara M, Ohsugi Y, Ogawa K, Okano H. Blockade of interleukin-6 signaling suppressed cochlear inflammatory response and improved hearing impairment in noise-damaged mice cochlea. Neuroscience Research. 2010; 66:345–352. [PubMed: 20026135]

Wan G, Corfas G. Transient auditory nerve demyelination as a new mechanism for hidden hearing loss. Nature Communications. 2017:8.

Wang Q, Hu B, Hu X, Kim H, Squatrito M, Scarpace L, deCarvalho AC, Lyu S, Li P, Li Y, Barthel F, Cho HJ, Lin YH, Satani N, Martinez-Ledesma E, Zheng S, Chang E, Sauve CG, Olar A, Lan ZD, Finocchiaro G, Phillips JJ, Berger MS, Gabrusiewicz KR, Wang G, Eskilsson E, Hu J, Mikkelsen T, DePinho RA, Muller F, Heimberger AB, Sulman EP, Nam DH, Verhaak RGW. Tumor Evolution of Glioma-Intrinsic Gene Expression Subtypes Associates with Immunological Changes in the Microenvironment. Cancer cell. 2017; 32:42–56e6. [PubMed: 28697342]

Willott JF, Bross L. Effects of prolonged exposure to an augmented acoustic environment on the auditory system of middle-aged C57BL/6J mice: cochlear and central histology and sex differences. J Comp Neurol. 2004; 472:358–70. [PubMed: 15065130]

Willott JF, Bross LS, McFadden S. Ameliorative effects of exposing DBA/2J mice to an augmented acoustic environment on histological changes in the cochlea and anteroventral cochlear nucleus. J Assoc Res Otolaryngol. 2005; 6:234–43. [PubMed: 15983726]

Yang S, Cai Q, Vethanayagam RR, Wang J, Yang W, Hu BH. Immune defense is the primary function associated with the differentially expressed genes in the cochlea following acoustic trauma. Hear Res. 2016; 333:283–94. [PubMed: 26520584]

Yang W, Vethanayagam RR, Dong Y, Cai Q, Hu BH. Activation of the antigen presentation function of mononuclear phagocyte populations associated with the basilar membrane of the cochlea after acoustic overstimulation. Neuroscience. 2015; 303:1–15. [PubMed: 26102003]

Young RW, Bok D. Participation of the retinal pigment epithelium in the rod outer segment renewal process. J Cell Biol. 1969; 42:392–403. [PubMed: 5792328]

Zhang C, Sun W, Li J, Xiong B, Frye MD, Ding D, Salvi R, Kim MJ, Someya S, Hu BH. Loss of sestrin 2 potentiates the early onset of age-related sensory cell degeneration in the cochlea. Neuroscience. 2017; 361:179–191. [PubMed: 28818524]

HIGHLIGHTS

- Lower level noise increases cochlear macrophage activity
- Lower level noise activates macrophage pro-inflammatory function in the cochlea
- Macrophages display reduced phagocytic activity following lower level noise stress
- Macrophage activation persists for an extended period of time after noise cessation

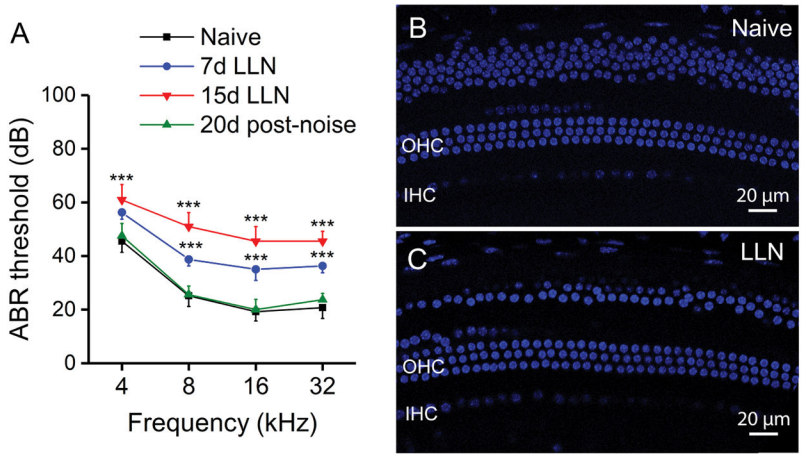

Figure 1.

ABR thresholds and sensory cells in naive and LLN exposed animals. ***A.*** ABR functional assessment in naive animals (n=10), animals exposed to LLN for 7 days (n=5) and 15 days (n=10), and animals tested 20 days following noise cessation (n=8). Compared to baseline measures under naive conditions, significant threshold shifts are observed at all tested frequencies at both 7 and 15 days with thresholds returning to baseline levels 20 days after noise cessation (*** $P < 0.001$). ***B.*** TO-PRO®-3 labeling of sensory cell nuclei in the basal turn of a naive CBA/CaJ mouse cochlea. ***C.*** Typical nuclear morphology in a cochlea examined following 15-day LLN exposure. Sensory cell nuclear integrity is maintained. The nuclei above the outer hair cells at the top of panels B and C are cells of Claudius. Many of these cells in panel C were not included when the OHC image was projected from a series of confocal images. OHC: outer hair cells. IHC: Inner hair cells.

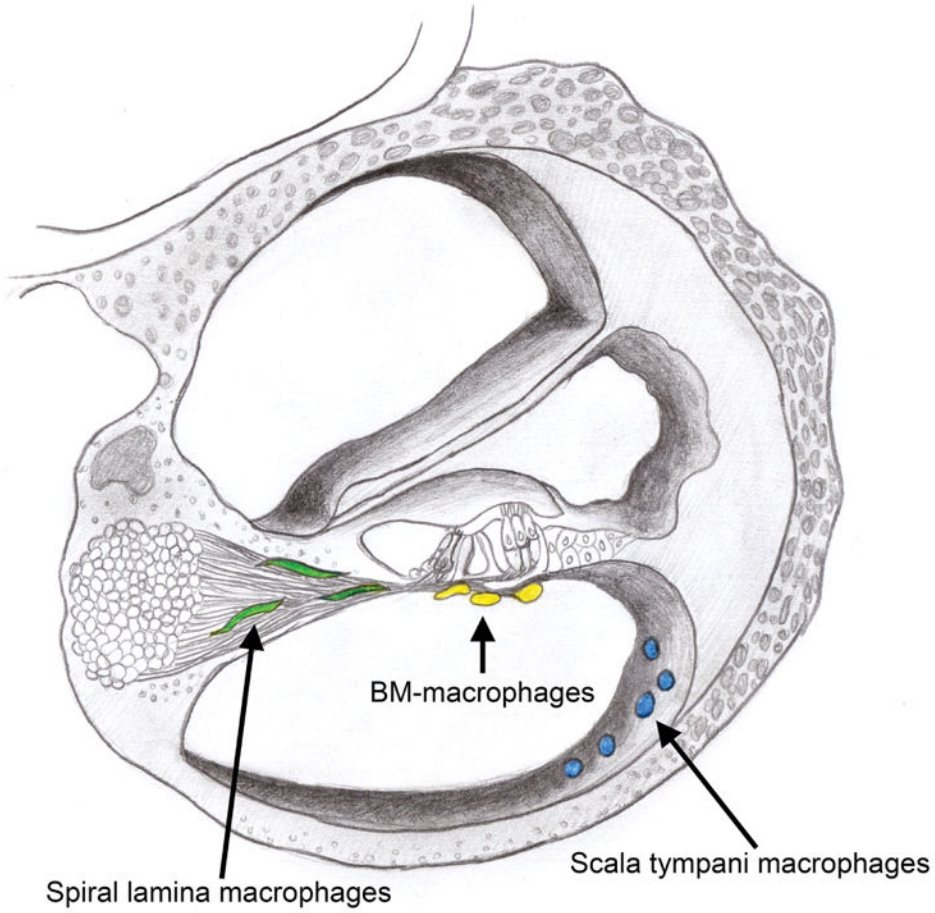

Figure 2.

Schematic drawing of a cochlear cross-section indicating the location of cochlear macrophages in three anatomic sites. The osseous spiral lamina macrophages reside closely among the peripheral fibers of the spiral ganglia and are color-coded green in this schematic. BM-macrophages inhabit the scala tympani cavity and are found immediately beneath the basilar membrane in close proximity to the sensory cells and their innervations by spiral ganglia (color-coded yellow). Cochlear macrophages on the luminal surface of the scala tympani cavity were also examined and are color-coded blue.

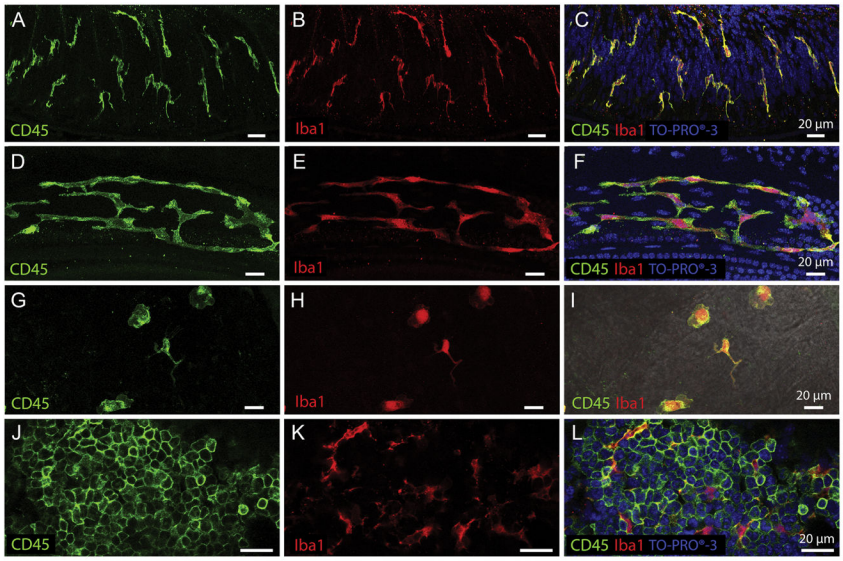

Figure 3.

Tissue macrophages display different morphologies in distinct cochlear partitions. ***A–C.*** Osseous spiral lamina macrophages residing among the peripheral nerve bundles of ganglion neurons. Under steady-state conditions, osseous spiral lamina macrophages present with a branched, dendritic morphology as revealed by CD45 (A) and Iba1 (B) immunolabeling. They are oriented radially toward the lateral edge of the osseous spiral lamina. To provide further context for immune cell analysis, tissues were counter-stained with TO-PRO®-3 (C). ***D–F.*** Steady-state BM-macrophages in the middle and basal cochlear region present as a network of long and thin curvilinear cells that follow the natural anatomic curve of the basilar membrane. BM-macrophages strongly express CD45 (D) and Iba1 (E) immunoreactivity. ***G–I.*** Macrophages on the luminal surface of the scala tympani in the basal turn of a naive cochlea. Under resting conditions, these cells present with a variety of morphologies (amoeboid to branched), are sporadically located among non-immune cells on the surface of the scala tympani, and possess both CD45 (G) and Iba1 (H) immunoreactivity. A merged image with CD45 and Iba1 colocalization can be seen in DIC view (I). ***J–L.*** CD45 (J) and Iba1 (K) immunohistochemistry performed on bone marrow harvested from the cochlear bony shell shows many small, rounded and undifferentiated leukocytes with very strong CD45 immunoreactivity (J). These small less-differentiated cells do not express the macrophage-specific protein Iba1. However, among the undifferentiated bone marrow leukocytes reside globular, branched, fully differentiated macrophages that express strong Iba1 immunoreactivity (K) indicating that only mature macrophages, but not less-differentiated leukocytes, express Iba1. CD45 and Iba1 colocalization with TO-PRO®-3 nuclear labeling can be seen in panel L.

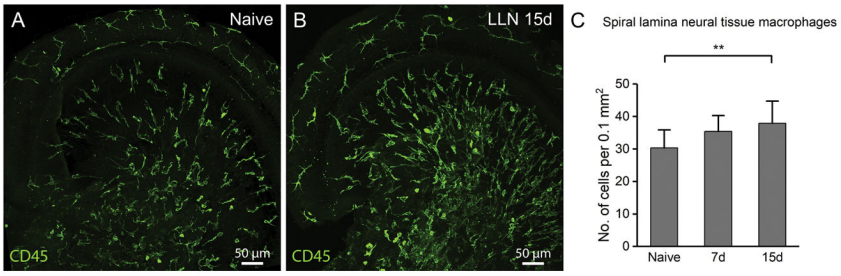

Figure 4.

LLN increases the number of osseous spiral lamina macrophages. ***A.*** Macrophages in the apical turn of a 2-month old cochlea under steady-state conditions. Note that immune cells run radially from the region of the modiolus toward the contact point between the osseous spiral lamina and the basement membrane of the basilar membrane. ***B.*** Apical turn of an age-matched cochlea exposed to LLN for 15 days. Following LLN, macrophages continue to be radially aligned along the spiral ganglion bundles, and the branched macrophage morphologies are maintained. However, their number is increased. ***C.*** Comparison of the macrophage numbers among naive cochleae (n=5) and those exposed to LLN for 7 days (n=5) and 15 days (n=5). A statistically significant increase in the number of osseous spiral lamina macrophages occurs following 15 days of LLN stress (** $P > 0.01$).

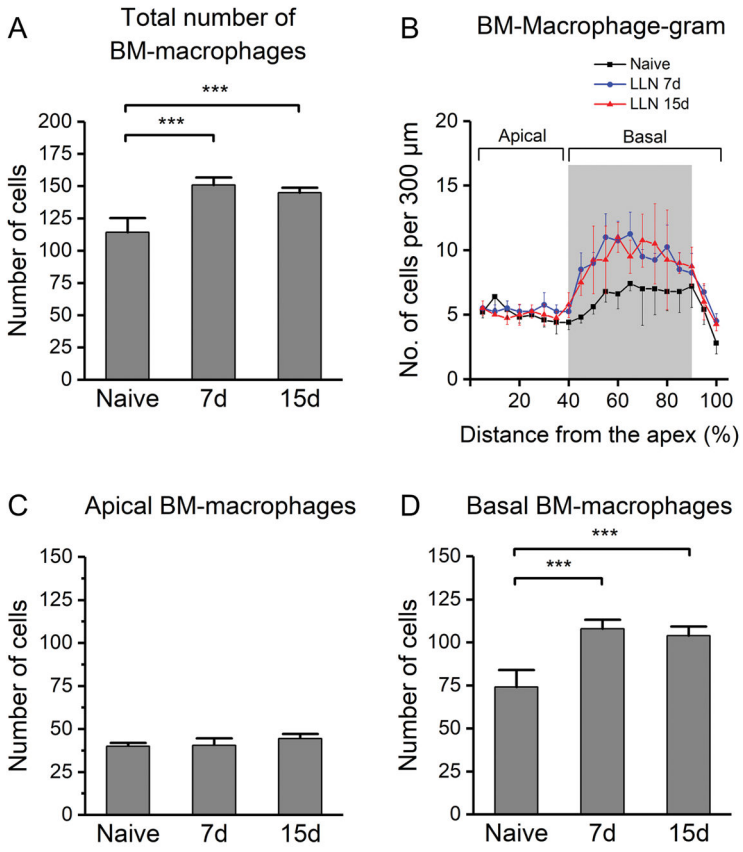

Figure 5.

Changes in BM-macrophage numbers following LLN exposure. Pre-noise: n=5, right after the noise: n=4, and 2 months after the noise: n=4. ***A.*** Comparison of the total number of macrophages across the entire length of the basilar membrane for naive cochleae and cochleae exposed to LLN for 7 days and 15 days. A statistically significant increase in the number of macrophages is observed for the 7- and 15-day groups as compared with the number of the control group (*** $P < 0.001$). ***B.*** BM-macrophage-gram showing the distribution of macrophages spanning the full length of the basilar membrane. Note the heterogeneous change in macrophage number in different regions of the sensory epithelium as a result of LLN exposure. ***C.*** Comparison of the total number of BM-macrophages in the apical section (0–40% distance from the apex) of the basilar membrane in naive (n=5) and LLN-stressed cochleae at 7 days (n=4) and 15 days (n=4). ***D.*** Comparison of the total number of BM-macrophages in the basal portion (40–100% distance from the apex). A substantial increase in the number of individual cells occurs subsequent to LLN stress, and this increase is statistically significant (*** $P < 0.001$).

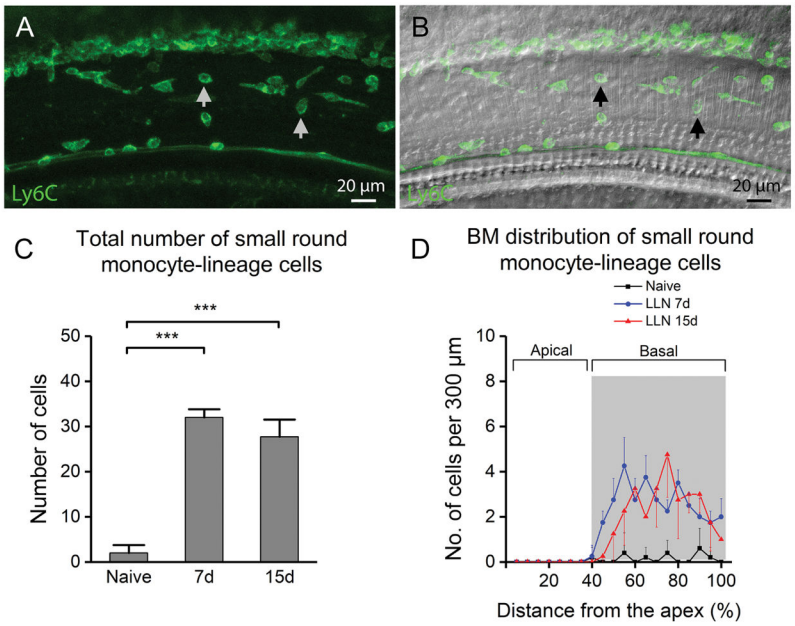

Figure 6.

Analysis of macrophages with a small round shape beneath the basilar membrane following LLN. ***A.*** A typical image of Ly6C-positive cells (pointed to by arrows) beneath the basilar membrane in the middle turn of a cochlea following LLN for 15 days. ***B.*** DIC view of the same cochlear site. ***C.*** The total number of small round Ly6C-positive cells increases following exposure to LLN (n=5 cochleae for each time point) (*** indicates $P < 0.001$). ***D.*** Distribution of Ly6C-positive cells along the basilar membrane. Note that the increase in the number of Ly6C-positive cells is specifically found within the middle to basal portion (40–100% from apex) of the basilar membrane of cochleae stressed by LLN. This cell type was comparatively scant in all basilar membrane portions of naive cochleae (data not shown).

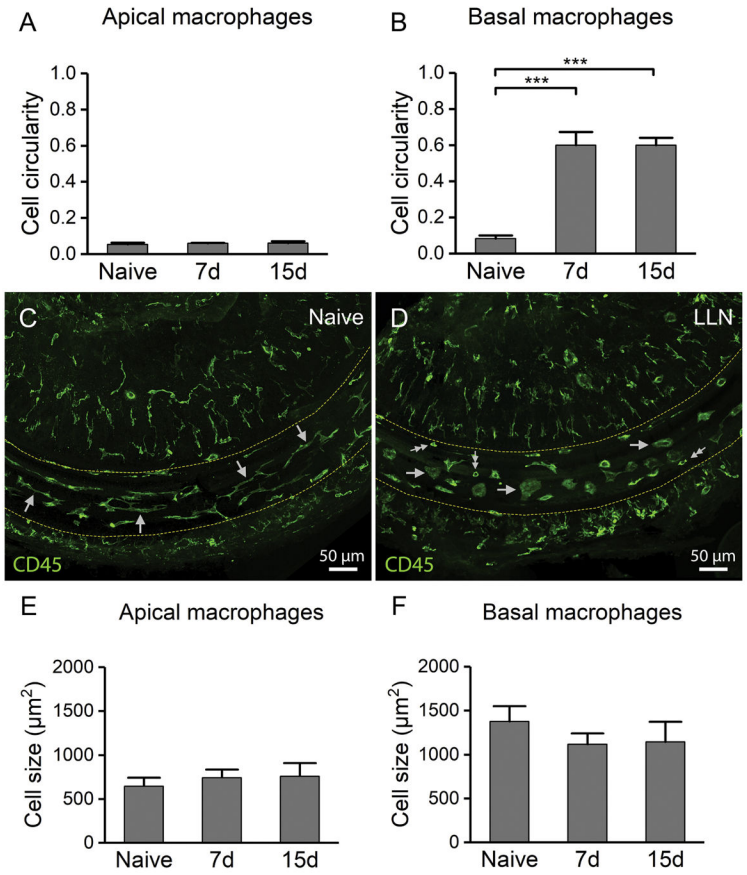

Figure 7.

LLN causes morphological transformation of BM-macrophages to activated phenotypes. ***A–B.*** Comparison of the circularity index of BM-macrophages between the naive cochleae (n=5) and the cochleae stressed with LLN for 7d (n=4) and 15 days (n=4). ***A***. Analysis of apical macrophages reveals the maintenance of the gross morphology subsequent to LLN. ***B.*** Morphological analysis of basal BM-macrophages reveals significantly more circular cell bodies in cochleae stressed with LLN for both 7 days and 15 days (*** $P < 0.001$). This change reflects the macrophage shape alterations from curvilinear networked cells in naive cochleae to rounded globular amoeboid macrophages dominant in cochleae stressed by LLN. ***C.*** Typical morphology of BM-Macrophages in the middle turn of a normal control cochlea. Note that under naive conditions, BM-macrophages in the middle turn appear as a network of long, thin curvilinear cells that are aligned with the natural curve of the basilar membrane (arrows). ***D.*** Morphology of macrophages in the same location of an age-matched cochlea exposed to LLN for 15 days. Macrophages transformed from a curvilinear networked shape seen under steady-state conditions to an amoeboid shape (large single arrows), a morphology associated with an activated immune status. In addition to large amoeboid cells, several small, round and teardrop shaped cells can be seen on the basilar membrane (small double arrows). ***E–F.*** Cell size comparison of BM-macrophages in naive cochleae (n=5) and cochleae exposed to LLN for 7 days (n=4) and 15 days (n=4). ***E***. Analysis of apical macrophages indicates no changes in cell size following LLN stress. ***F.***

Size analysis of basal BM-macrophages reveals a slight decrease in the mean cell size subsequent to LLN stress, but the change is not statistically significant.

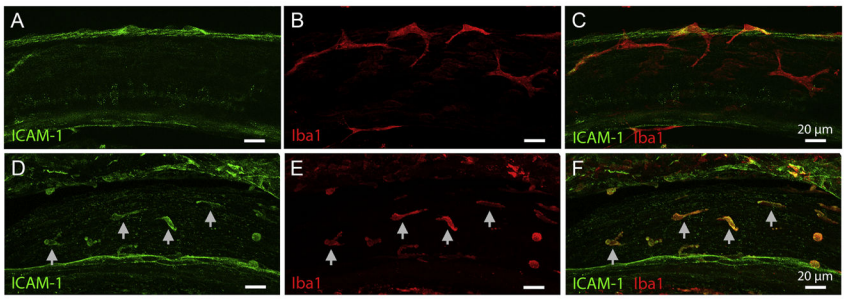

Figure 8.

LLN enhances the ICAM-1 expression in BM-macrophages. ***A–C.*** ICAM-1 immunoreactivity is scant in naive BM-macrophages. ***D–F.*** ICAM-1 immunoreactivity is enhanced following LLN stress. Arrows point to ICAM-1 positive cells that display strong Iba1 immunoreactivity.

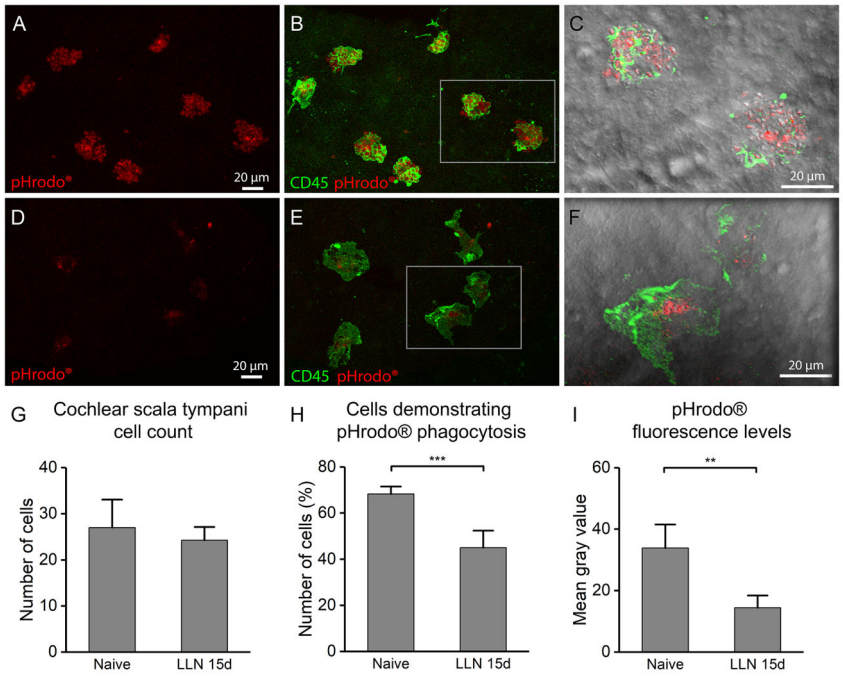

Figure 9.

Reduction of macrophage phagocytic ability after LLN exposure. ***A.*** Robust zymosan bioparticle fluorescence within the cell bodies on the luminal surface of the scala tympani cavity in a naive cochlea. ***B.*** Cells that contain zymosan bioparticles display strong CD45 immunoreactivity and have a rounded morphology with an uneven texture due to the large number of bioparticles phagocytized by these cells. ***C.*** Enlarged DIC view of inset (from panel B) reveals the bulging, bumpy surface of these cells with many small, granulated bioparticles visible within the cell bodies. ***D.*** Very weak and limited bioparticle fluorescence within the cell bodies of scala tympani macrophages in a cochlea stressed with LLN for 15 days. Substantially reduced fluorescence can be observed compared to the fluorescence observed in the control ear (A). ***E.*** Double-staining of the same tissue for CD45 showing the lack of rough texture as seen in the control ear (B). ***F.*** DIC view of inset (enlarged from panel E) reveals that LLN-stressed macrophages have ingested far fewer bioparticles compared to the resting cells in naive ears (C). ***G–I.*** Analyses of macrophages on the luminal surface of the scala tympani in naive cochleae (n=4) and cochleae stressed with LLN for 15 days (n=4). ***G.*** Quantification of the number of macrophages revealed a slight, but not significant reduction in cell number following LLN stress compared to naive controls. ***H.*** Comparison of the proportion of macrophages containing bioparticle fluorescence to the macrophages that lack the bioparticle fluorescence reveals a significantly reduced number of cells engaging in phagocytosis in ears stressed with LLN compared to naive ears (*** $P < 0.001$). ***I.*** Comparison of the bioparticle fluorescence intensity as measured in macrophages participating in any degree of phagocytosis reveals significantly reduced fluorescence in LLN-stressed ears compared to naive controls (** $P < 0.01$).

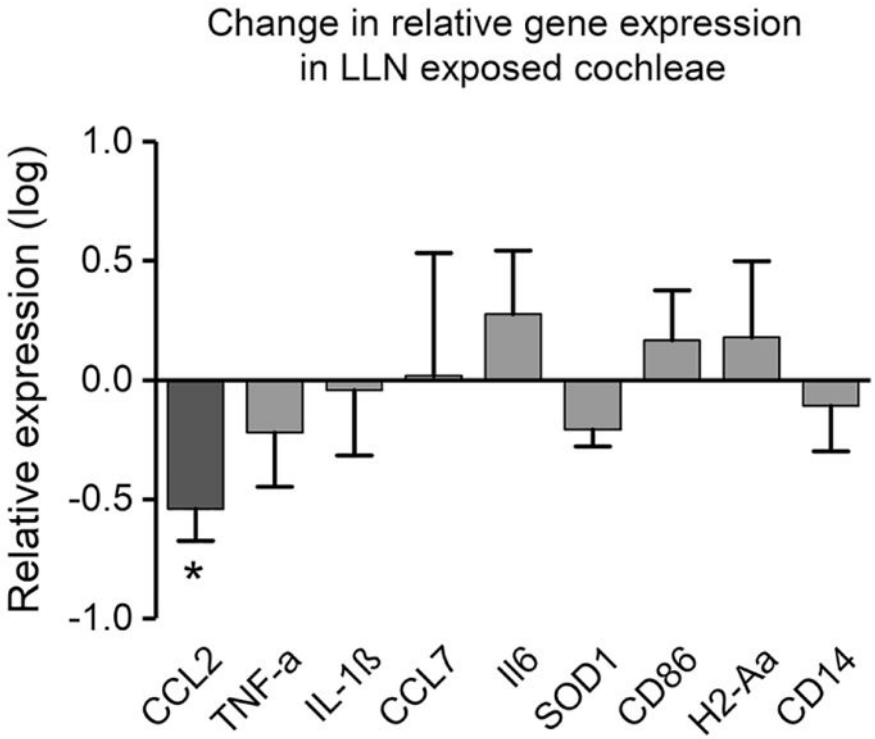

Figure 10.

Analysis of transcriptional expression of immune associated genes in the cochlear tissues collected from control cochleae and cochleae that sustained LLN for 15 days. No significant changes are present for all examined genes except for CCL2, which displays a slight reduction after LLN (* $P < 0.05$) (n=4 biological replicates for both the control and the LLN group).

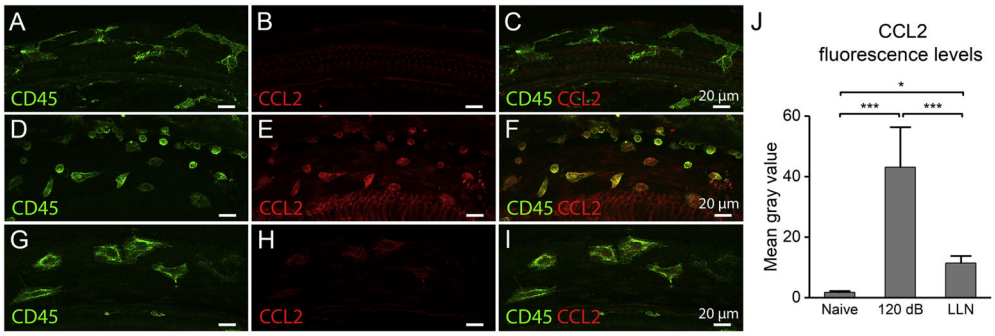

Figure 11.

CCL2 immunoreactivity in BM-macrophages at resting conditions, after exposure to a traumatic noise at 120 dB SPL for 1 hour, and after exposure to LLN for 15 days. ***A–C.*** CCL2 immunoreactivity in basal BM-macrophages of a naive control ear. Panel A shows CD45 immunoreactivity, panel B shows CCL2 immunoreactivity and panel C shows the merged view of panels A and B. Note that CCL2 immunoreactivity is very weak in steady-state macrophages (B). ***D–F.*** CCL2 immunoreactivity after a 120-dB noise exposure for 1 hour. A large number of smaller round to teardrop shaped cells are present and these cells display very strong CCL2 immunoreactivity, suggesting that exposure to traumatic noise increases the expression of CCL2. ***G–I.*** CCL2 immunoreactivity in basal BM-macrophages of a cochlea that sustained LLN for 15 days. Panel G shows CD45 immunoreactivity, panel H shows CCL2 immunoreactivity and panel I shows the merged view of panels G and H. Following LLN stress, basal BM-macrophages exhibit amoeboid morphologies and a weak CCL2 immunoreactivity. ***J.*** Comparison of the CCL2 fluorescence levels in BM-macrophages among the naive group, the 120-dB noise group and the LLN group. The 120-dB noise group displays a marked increase in CCL2 immunoreactivity as compared to the naive control group. The LLN group also displays an increase, but the level of the increase is significantly less that that seen in the 120-dB noise group (*** $P < 0.001$; * $P < 0.05$).

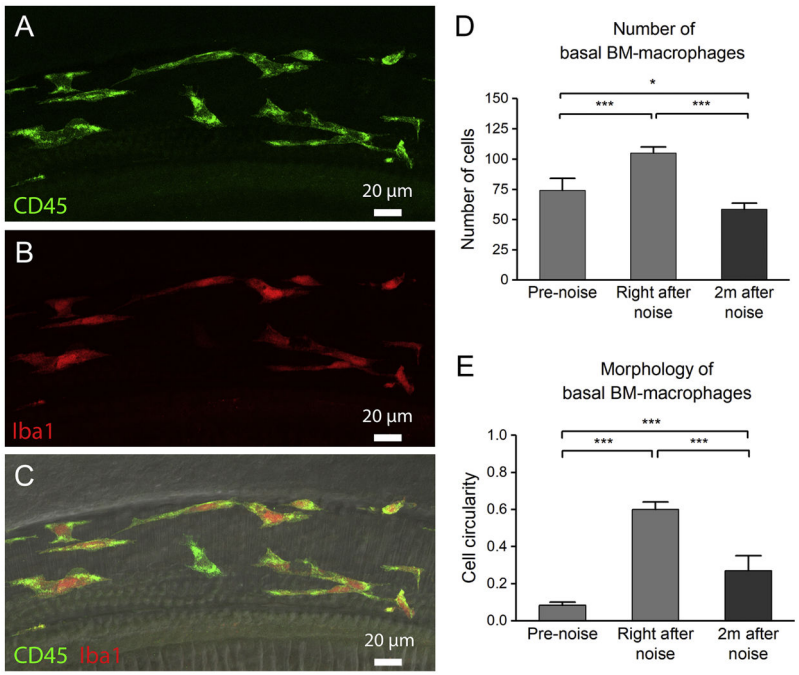

Figure 12.

Partial return of activated macrophage morphology 2 months after 15-day LLN. ***A–C.*** Typical morphology of BM-macrophages 2 months after noise exposure cessation. Panel A shows CD45 immunoreactivity, panel B shows Iba1 immunoreactivity and panel C displays a merged view of panels A and B together with DIC view of the same region. At this time point, basal BM-macrophages have begun to return to a more branched morphology with shorter processes, distinct from the very amoeboid morphologies observed immediately after LLN. ***D.*** Comparison of the number of basal BM-macrophages at three time points. A biphasic change in the number of basal BM-macrophages is observed with an initial increase from the starting level of 74 ± 10 cells to 105 ± 5 cells immediately after the noise exposure and then a subsequent decrease to 58 ± 5 cells observed 2 months after noise cessation (*** P <0.001; * P < 0.05). n=4 for each time point. ***E.*** Morphology of basal BM-macrophages at three time points using a cell circularity index. Notice that by 2 months after noise cessation, basal BM-macrophages have reduced circularity compared to the degree of circularity right after the noise. However, the value of the circularity has not returned to the pre-noise level (*** P < 0.001). n=4 for each time point.